Supporting Materials

Appendix A1: Demographic and spatial model specifications

Prairie Dog Metapopulation Model

Spatial structure of study region

The spatial structure of the metapopulation was based on the distribution of prairie dogs in the Conata Basin, a subset of 71 prairie dog populations within the Conata/Badlands region in South Dakota and covering ca. 500 km^2 (Fig. 1; delineated based on Biggins et al. 2011) is a portion of the Buffalo Gap National Grasslands directly south of Badlands National Park and is administered by the US Forest Service (Fig. 1). This area was chosen in the early 1990's for reintroduction of black-footed ferrets due to the extensive network of high-density prairie dog colonies located on public lands (Livieri 2006). As part of black-footed ferret reintroduction efforts, 150 captive-born ferret kits were released over a 4-year period to prairie dog colonies in Conata Basin beginning in 1996. This effort resulted in a self-sustaining population with an annual total of approximately 200 animals by the year 2000 (Livieri 2006). Plague-free prairie dog populations at Conata Basin contributed to rapid establishment of ferrets at this site, making it among the most successful ferret reintroduction sites and the largest reintroduced population of black-footed ferrets (335 individuals recorded in 2007). The black-footed ferret population at Conata Basin has declined dramatically since sylvatic plague was detected in 2008, falling from 335 individuals documented in 2007 to only 71 in 2012 (Livieri et al. *in prep*).To prevent extinction of the ferret population, plague mitigation efforts have recently been implemented, including dusting of prairie dog burrows and experimental vaccination of black-footed ferrets (Abbott and Rocke 2012).

Prairie dog colonies in Conata Basin, Badlands National Park, and Buffalo Gap National Grasslands in southwestern South Dakota, USA (hereafter, Conata/Badlands region) were mapped biennially by the US Forest Service and Badlands National Park from 1996-2009 using differentially corrected Global Positioning Systems (GPS) units to connect the outermost prairie dog burrows into a polygon (Biggins et

al. 2006a). Prairie dog colonies in the surrounding areas were mapped in 2004 using aerial transects and digital imaging (Sidle et al. 2001, Cooper and Gabriel 2005). We converted prairie dog colony maps to binary (0=non-habitat, 1=habitat) raster maps with 50m cell size. We re-imposed barriers (e.g., roads, pipelines) that were lost in the rasterization process. We used the union of all years to define potential habitat. We used neighborhood distance of 1 cell (50m) to define the population structure (see Akçakaya 2002 for details of how the program determines spatial structure). Thus, we assumed each colony is a distinct biological population, which may be connected to other such populations (see section on dispersal below). Excluding very small colonies with carrying capacity (*K*) <100 (see below), this resulted in 1591 PD populations ranging from about 5 ha to 10,000 ha, with a median size of 16 ha (Fig. A1-1). Finally, we used the union of the mapped polygon boundaries from all surveys 1996-2009 to define the spatial extent of all distinct prairie dog colonies within the region, resulting in a metapopulation of 1591 black tailed prairie dog colonies ranging from ca. 5 ha to 10,000 ha in size (median colony area of 16 ha; Fig. A1-1) and covering ca. 20,000 km^2.

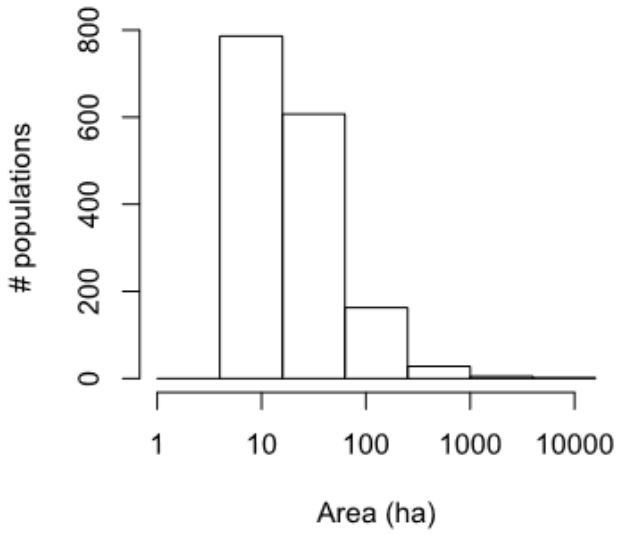

Fig. A1-1. Histogram of patch areas (ha) for all prairie dog habitat patches (n = 1591) identified in the Conata-Badlands region of South Dakota, based on mapped records of prairie dog colony boundaries.

Carrying capacity and density dependence

Reproduction in prairie dogs is often limited by resources (Hoogland 2001), suggesting a Ricker-type (scramble) density dependent effect on fecundities. We therefore used this type of density dependence, and estimated the maximum growth rate (R_{max}) based on the average of exponential growth rates exhibited by several populations following crashes. Three of these rates were following crashes due to plague: 1.466 (Biggins et al. 2006a, Fig 6.4), 2.024 (Cully and Williams 2001, Fig 4, years 1989-1991) and 3.806 (Cully and Williams 2001, Fig 4, years 1995-1997). We combined these rates with four growth rates following crashes due to other causes, including shooting, toxicants and removal and translocation (Reeve and Vosburgh 2006, Table 10-3, excluding the lowest and highest rates, which were from populations that had not undergone a recent population reduction). The average of these 7 exponential growth rates was 2.44. For sensitivity analysis, we used the quartiles, giving a range of 1.8 to 2.8. These values coincided with an independent estimate based on the intercept of the regression of population growth rate (R) on population size (N) from the data of Hoogland (1995, Table 16.1), which gave s estimates of 2.4 to 3.7, depending on the type of regression. Given that regression of R on N often overestimates R_{max}, this range is consistent with the estimate based on exponential growth phases of the two populations mentioned above.

We assumed each mapped colony (see above) represented a distinct biological population, with carrying capacity (K) defined as a function of colony area and average densities of prairie dogs. At Conata Basin, the average density of prairie dogs prior to the arrival of plague was 28.7/ha (Livieri 2006). Thus, we multiplied the number of cells in each patch with 7.175 (=28.7*0.25) to calculate the carrying capacity of that patch (because under the Ricker-type density dependence we used, average abundance would approximately equal the equilibrium abundance or carrying capacity). Colonies with K<100 were excluded from analysis, to decrease the number of populations and because very small populations do not contribute substantially to population dynamics. We assumed initial abundances were equal to K for each population, and we ran a 10-year burn-in period for all simulations to ensure that all colonies were at equilibrium with their environment and had reached a stable age distribution.

Demographic structure and vital rates

We developed an age- and sex-structured matrix model for prairie dogs using RAMAS Metapop software (v. 6.0; Akçakaya and Root 2013), with eight female and six male age classes, parameterized using

survival rates and fecundities drawn from Hoogland (2001). We parameterized the matrix according to a pre-breeding census. We used survival rates based on Hoogland (2001, Figs. 1a and 2a), and fitted a polynomial regression of survival rate vs. age for each sex to obtain a smooth function of age (Fig. A1-2). We calculated litter size as 3.1 (from Hoogland 2001, figure 3a). Combining this value with proportion of females breeding (0.43; Hoogland 2001), and survival rate of zero-year olds, we estimated fecundity as 0.418 daughters and 0.379 sons per adult female (age 2+) and 0.209 daughters and 0.189 sons per yearling female (age 1). We assumed polygynous mating system with each male mating with up to 4 females. Because the density dependence function modifies the stage matrix as a function of population size, the model results would be sensitive to the R_{max} value of the density-dependence function, not to the exact vales of survival rates and fecundities. Therefore, the sensitivity to vital rates was modeled through the R_{max} sensitivity (see section on sensitivity analysis, below). All colonies were initialized at K and at stable age distribution, and all simulations were run with a 10 year burn-in period (to reach approximate equilibrium in the prairie dog metapopulation).

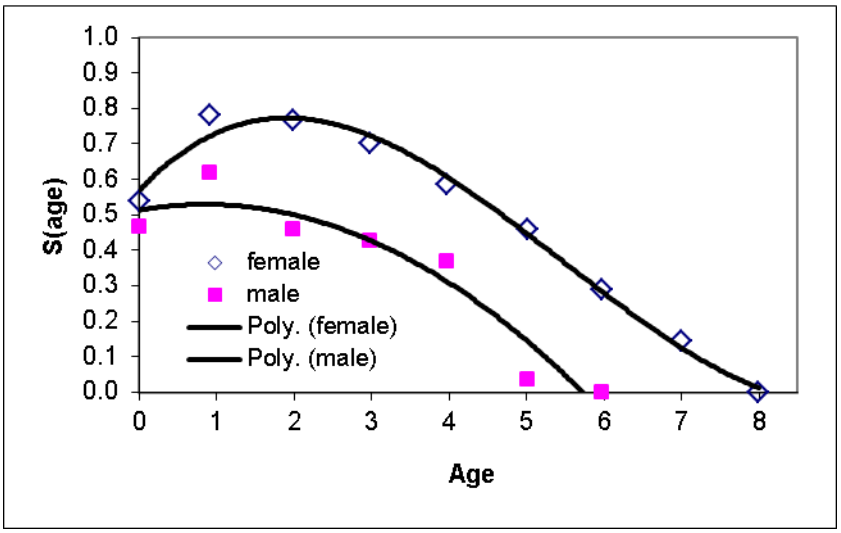

Figure A1-2. Illustration of polynomial regressions used to estimate expected age-specific survival rates for prairie dogs in this study, based on Hoogland (2001).

Variability

The temporal variation in vital rates is based on 14 years of age and sex-specific census data from Hoogland (1995, Table 16.1, page 377). It is important to note that the censused population has fluctuated between 150 and 250 individuals and does not seem to have crashed because of plague or other reasons during the study period (otherwise, adding disease dynamics would overestimate variability). In order to obtain environmental variability, we removed demographic variance from observed variance of survival rates and fecundities, based on expected binomial and Poisson variance (Akçakaya 2002), and calculated coefficients of variation (Table A1-1). For sensitivity analysis, we used minimum and maximum values based on bootstrapping (Table A1-1).

Table A1-1. Coefficients of variation (CV) for survival rates and fecundities of males and females and minimum and maximum values of CVs based on bootstrapping

Vital rate	sex	CV	min CV	max CV
Survival rate	Female	0.111	0.102	0.119
	Male	0.185	0.136	0.201
Fecundity	Daughters	0.350	0.303	0.376
	Sons	0.291	0.268	0.331

Plague

We modeled plague dynamics within the prairie dog metapopulation as catastrophes spread by dispersers, with virulence (overall survival) and per-disperser probability of initiating an outbreak estimated from the Outbreak epidemiological model described below (n = 1000 replicates). We calculated the probability that a disperser initiates a catastrophe in the target population by multiplying the year-averaged probability that an individual (in a population that is experiencing an outbreak) is in disease state E (infected but not yet infectious), with the probability that a single individual in disease state E initiates an plague epizootic that kills at least half of the population. Specifically, the Outbreak model indicated a 9.3% chance of an individual disperser being capable of initiating plague in a new colony (averaged over an entire year, a prairie dog capable of dispersal from an infected colony had a 9.3% chance of being an exposed carrier), and a 97% chance that such a disperer would initiate a

catastrophe, resulting in a 9% per-disperser chance of initiating a catastrophe. When a catastrophe does get an initiated in a population, the survival rate is determined, according to the Outbreak results, as 2.9% survival (97.1% mortality) in the year that plague is initiated (with no long-term effects). We initiated the plague outbreak in year 11, following a 10-year plague-free period (in turn, following the 10-year burn-in period). reflecting ca. ten plague-free years at Conata Basin following the first ferret introductions (sylvatic plague was first detected in the Conata Basin in May 2008; Abbott and Rocke 2012). Plague was initiated in the prairie dog metapopulation assuming either (1) plague was initiated in a single randomly selected prairie dog population (selected from among mid size or larger populations in the Conata Basin), or (2) plague outbreaks arise spontaneously with a probability of 0.005 per year per colony (effectively resulting in spontaneous plague initiation events somewhere in the metapopulation nearly every other year). Because RAMAS Metapop computes the number of dispersers based on post-plague abundances, we also computed the mean number of infected (exposed) dispersers as a function of the final colony abundance, resulting in an estimate of 118% (SE 28%). Therefore, we set the "probability of infection per disperser" parameter in Ramas Metapop at its maximum value of 100% (thereby potentially underestimating the rate of spread).

Dispersal

Dispersal rates (proportion of individuals dispersing between each pair of defined populations) were modeled as a function of centre to edge distances between populations, in order to avoid very large populations flooding small populations around them. Dispersing prairie dogs traveled a mean straight-line distance of 2.4 km (Garrett and Franklin 1988). Maximum dispersal distance is 10 km (Knowles 1985 cited in Knowles et al. 2002; Lomolino and Smith 2001). Thus, we used a dispersal-distance function

$$a \exp(-D/b) = 0.083 \exp(-D/2.4),$$

where D is distance from the centre of the source population to the closest edge of the target population, with a maximum dispersal distance of D_{max} = 10 km. We calculated the intercept (the a parameter) as follows. Based on the spatial structure of populations, we calculated the average number of neighbors at distances of 0-0.5 km, 0.5-1 km, 1-2.5 km, 2.5-5 km and 5-10 km. We set the intercept such that the total expected rate of dispersal from this average population was about 0.37, which was

138 calculated as the product of two numbers: (1) 59% of yearling males dispersing from a study population
139 (based on data reported in Tables 1 and 2 in Garrett and Franklin 1988), and (2) relative survival rate of
140 dispersers (calculated as 0.62, based on survival rate of 0.9 and 0.56 of residents and dispersers as
141 reported by Garrett and Franklin 1988). For the spatial sensitivity analysis, we used a range of 0.061 to
142 0.105 for the *a* parameter, based on ± 0.10 for the total expected rate of dispersal from the average
143 population.

144 The above calculation refers to dispersal rate of yearling males. We calculated the relative dispersal of
145 other age/sex classes as 0.46 for yearling females, 0.1 for adult males and 0.39 for adult females (based
146 on data reported in Tables 1 and 2 in Garrett and Franklin 1988). These numbers are consistent with
147 general observations of age- and sex-specific dispersal: Hoogland (1995) reported that female prairie
148 dogs usually remain with their natal coterie, or they disperse long distance to other colonies, but "short-
149 distance dispersal of females within the home colony almost never occurs" (p.383); male prairie dogs,
150 on the other hand, disperse either long-distance to new colonies (mostly as yearlings, rarely as adults) or
151 short-distance within the home colony.

152 ***Correlation***

153 Correlation of population dynamics among populations was based on a function of center-to-center
154 distances between populations. Because annual fluctuations in vital rates are likely a function of
155 weather conditions, we used temporal correlation in weather conditions as a proxy for describing
156 correlation of population fluctuations. Specifically, spatial autocorrelation in vital rates was modeled as
157 a function of inter-colony distances based on 30 years of summer rainfall data from 15 sites randomly
158 drawn from within the range of the black-tailed prairie dog. We fit a negative exponential model using
159 30 years of summer rainfall data drawn from 15 random locations in the southwestern quarter of South
160 Dakota (PRISM dataset; PRISM Climate Group, Oregon State University, http://prism.oregonstate.edu).
161 The resulting equation, correlation= $\exp(-D/601)$, where D is the distance between populations, was
162 used for all model runs and was not modified as part of spatial sensitivity analyses (Fig. A1-3).

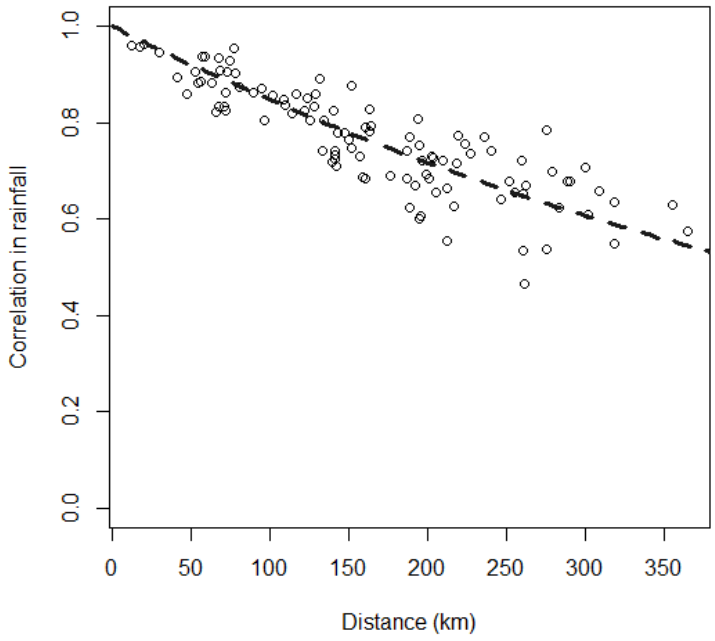

Figure A1-3. Illustration of the correlation-distance function used for all prairie dog models in this study. Spatial correlation in rainfall was assumed to correspond more generally to spatial correlation in environmental variation.

Black-footed Ferret Population Model

Demographic structure and vital rates

We developed an age- and sex-structured matrix model, with 5 female and 5 male age classes. We parameterized the matrix according to a post-breeding census, with survival rates drawn from a Wyoming mark recapture study (Grenier 2008). Juvenile (first year) and adult (yearling and above) survival rates were set at 0.39 (SE 0.17) and 0.67 (SE 0.15), respectively. For sensitivity analysis, we used a range of 0.22 to 0.56 for juvenile survival rate, and 0.52 to 0.82 for adult survival rate, representing one standard error from the mean. Juvenile and adult fecundity were set at 0.73 and 1.25, respectively, based on observations of kits produced from 2004-2006 (Grenier 2008). For sensitivity analysis, we used a range of 0.36 to 0.92 for juvenile fecundity and 0.86 to 1.35 for adult fecundity.

Density dependence, carrying capacity, and initial abundances

The strong dependence of Black-footed Ferrets on Prairie Dogs as prey suggests density dependence based on resource limitation and linked to resource (prey) dynamics. We therefore modeled Black-footed Ferret density dependence with a Ricker-type density dependence, corresponding to a scramble competition model (Brannstrom and Sumpter 2005).

We ran the black-footed ferret population model assuming either (1) ferrets could only access prairie dog colonies within the Conata Basin, or (2) ferrets could access all 1591 prairie dog colonies within the Conata/Badlands region. In the former case, we assumed the ferrets could only access PD colonies within the Conata Basin, a region of approximately 13,000 ha which we delineated as the aggregate of the three ferret subunits identified in Biggins et al. (2011). Thus, although the PD/plague model (see above) covered a larger area of southwestern South Dakota, only those populations in the Conata Basin were linked to the black-footed ferret model. Because ferret populations were rapidly extirpated by plague if limited to the Conata Basin proper, and because the maximum possible spatial extent for black-footed ferret populations is unclear (see main text), we also ran scenarios in which all prairie dog populations in the Conata-Badlands region were assumed to be available to the ferrets as prey.

We calculated the black-footed ferret functional response based on the energy balance model of Stromberg et al. (1983), using median requirement of equilibrium population size of 766 PD to support one black-footed ferret at a R = 1, thereby equating to the equilibrium N of the scramble function in RAMAS Metapop. Thus, carrying capacity (*K*) of the black-footed ferret population was calculated as 1/766 of the PD population size in Conata Basin at each time step. However, in years of high prairie dog abundance, ferrets typically maintain territories supporting more prairie dogs than they need to survive (Biggins et al. 2006b). In other words, the linear relationship between prairie dog density and black-footed ferret carrying capacity breaks down at high prairie dog densities. We capped the value of *K* at 462 for the Conata region based on the maximum ferret density of 0.04 ferrets per ha suggested by Biggins et al. (2006b). For global sensitivity analysis, we similarly capped the value of *K* to maintain a maximum density of 0.04 ferrets per ha (therefore, *K* varied based on landscape extent). Thus, even in years when prairie dog abundance is very high, the carrying capacity of the ferret population does not exceed the maximum limit dictated by territoriality.

We set the maximum growth rate (R_{max}) to 1.48, based on the average of two estimates of the rate of (exponential) growth in a Wyoming population (Grenier et al. 2007). One estimate is 1.35, the eigenvalue of the matrix fitted to mark-recapture data, and the other estimate is 1.60, the (scalar) rate of growth in the minimum number of live ferrets from 2000 to 2006. For sensitivity analysis, we used these two values.

Black-footed ferret abundance for each iteration was initialized using known reintroduction events in the Conata Basin , as described by Livieri (2006; i.e., dates and ages of releases were modeled explicity). Ferret population viability was summarized using three metrics: quasi-extinction risk (defined as the proportion of simulation runs falling below 5 individuals at year 60 of the simulation), expected minimum abundance (defined as the minimum abundance after year 10 of the trajectory averaged over all 1000 simulations; McCarthy and Thompson 2001), and mean final abundance (at year 60).

Variability

We estimated temporal variability in ferret vital rates (i.e., variability not due to fluctuations in the prey base, which was modeled explicitly via variation in *K*) by running the linked ferret/prairie dog metamodel for Conata basin under plague-free conditions and adjusting the ferret temporal variability parameter to match the observed annual variability from the re-established ferret population in the Conata Basin (Livieri 2006). Although most of the variability in black-footed ferret populations is likely due to variation in the prey base (here translated into variation in *K*), variability in other environmental factors may contribute to variability in black-footed ferret vital rates. To estimate the magnitude of this contribution, we created a retrospective model of the growth of the Conata Basin black-footed ferret population from 1996 (shortly after its introduction) until 2007 (before the first plague outbreak) based on Livieri (2006). We reconstructed the Conata reintroduction effort using RAMAS Metapop, using management events (introduction and harvest) to schedule the history of ferret introductions and translocations described by Livieri (2006). We ran the simulations with demographic stochasticity, vital rates specified as above, and carrying capacity linked to natural temporal variability in plague-free prairie dog population density (see above). Variability in black-footed ferret population growth in the early years of the Conata reintroduction program was likely related to different release strategies and predator exclusion measures (Livieri 2006). Ferret releases largely ended in 1999, and therefore we assumed that population variability observed from 2001 through 2007 (prior to sylvatic plague

234 epizootic) were due primarily to natural variability. Holding all other sources of variability constant
235 (demographic stochasticity and variability in prey abundance), we adjusted the coefficient of variation
236 for environmental variation in black-footed ferret vital rates so that the median simulated population
237 variance (computed as the variance of (N_{t+1}/N_t), n = 1000 simulations) matched the observed variability
238 in the Conata time series. The CV value that best fit the observed Conata time series was 11.5%, and this
239 value was used to compute temporal process variation for all vital rates. For sensitivity analysis, the CV
240 for ferret vital rates varied between 5 and 16%, which was the range of CV values for which the
241 observed variability fell within the interquartile range from the simulations.

242 ***Sensitivity to uncertainty in vital rates***

243 Sensitivity analysis results are not presented for the black-footed ferret population model, since the
244 main objective of this project was to assess the sensitivity of the ferret population to plague dynamics
245 across a variety of realistic prairie dog-occupied landscapes (see main text and Appendix C). However,
246 the simulation results were nearly identical across the plausible range of values for R_{max} and
247 environmental variability (described above). This insensitivity of ferret extinction risk to ferret vital rates
248 was due to the strong (nearly exclusive) dependence of ferret extinction risk on minimum landscape-
249 level prairie dog abundance (see text; Fig. A4-6).

250

Appendix A2: Details on the plague transmission model used to inform plague spread among prairie dog colonies

Background

Sylvatic plague, caused by the bacterium *Yersinia pestis,* is an exotic vector-borne disease of wild rodents that was introduced to western North America near the start of the 19th century (Link 1955) and became widespread across the western states by the mid-1900s (Eskey and Haas 1940; Barnes 1982). It is now maintained in enzootic cycles within rodent populations throughout much of the semi-arid prairie biome (Barnes, 1993). This bacterium is highly transmissible by infected fleas (Poland and Barnes, 1979) and causes a rapidly fatal disease in prairie dogs (Barnes, 1993; Cully and Williams 2001). Since the arrival of plague, devastating epidemics in prairie dog populations have been described (Lechleitner et al, 1968, Gage and Kosoy 2005, Cully et al. 2010, Cully and Williams 2001, Ecke and Johnson, 1952). Plague epizootics occur variably every 5-10 years in affected prairie dog systems (Barnes, 1982) and can reduce colony size by >90% and disrupt mesocolony structure (Cully et al., 2010).

Sylvatic plague now affects much of the prairie region of the USA, presenting a clear challenge to the future of black-footed ferret reintroduction efforts (Livieri 2011). As the sole food source for the black-footed ferret, the impact of this disease on prairie dogs has limited the conservation of the black-footed ferret and consistently hampered attempts to reintroduce this endangered species to its former habitats. Consequently, control of plague outbreaks in prairie dog populations is an important conservation issue and has recently been incorporated into the Black-footed ferret Species Survival Plan (SSP).

We developed an individual-based epidemiological model based on comprehensive literature review of published field and laboratory data that simulated plague spread through a prairie dog colony (see below). Simulation of basic epidemiological processes and reporting of survival states was done at a daily time step using the software Outbreak version 1.0 (Pollak et al. 2008; Lacy et al. 2012). We used an Outbreak extension called Infector to accommodate plague spread through spatially structured prairie dog colonies (black-tailed prairie dog colonies consist of loosely connected collections of family groups, called coteries; Hoogland 2001). The capabilities of Infector have since been added to Outbreak version

2, available at www.vortex10.org/Outbreak.aspx. Outbreak models (n = 5000 iterations) were initialized with a single infected individual within a colony size of 1000 individuals, and all simulations were run for 365 days. Although there is some evidence for resistance to Y. pestis in black tailed prairie dogs (Rocke et al., 2012; Pauli et al. 2006), we chose not to model this because it is not yet well understood and therefore difficult to parameterize. Simulated epizootic dynamics and population outcomes were compared to known field observations of prairie dog populations in plague-endemic areas to validate the model. Outbreak output tables were used to generate three summary statistics that were subsequently used for modeling prairie dog metapopulation dynamics: (1) Overall survival rate in a plague outbreak year, (2) probability of a potential disperser individual being a carrier of plague, and (3) the probability of a single infected individual initiating a population-wide outbreak. Details of the Outbreak model is provided below.

Disease is introduced by initializing the population in Vortex, with one animal initially infected (disease state E), and all others susceptible. Hence, on day 1, an infected prairie dog (defined as exposed in Outbreak) is introduced and becomes infectious after the required incubation period of 4-21 days. Once the individual transitions to infectious, s/he is capable of transmitting the disease agent and the plague outbreak is initiated. The dynamics of a plague epizootic are modeled as 365 days in Outbreak (with Infector). Vortex is used to initialize the population for MetaModel Manager (including disease state and coterie membership on an X-Y grid), but was not otherwise used in this initial model used to obtain disease parameters.

Initial population distribution among coteries (Infector specification)

Prairie dog coteries (family groups on a territory) are typically about 15 animals. The initial animals (*n* = 1000) were therefore assigned randomly to a 6x10 grid of territories. The exact age and sex distribution within these coteries does not affect the Outbreak model, because disease transmission was not modeled as being age or sex-dependent.

Disease transmission model

Transmission of *Y. pestis* was modeled as a combination of three different transmission mechanisms to capture the differential rates of disease transmission among coterie members, between adjacent coteries, and more distantly to prairie dogs in non-adjacent coteries.

- Transmission among coterie members was modeled with the "Within-group" transmission of Infector.
- Transmission between prairie dogs belonging to adjacent coteries (defined as those at X-Y coordinates within 1 in any direction from the focal coterie) was modeled with the "Between-group" transmission of Infector.
- Transmission between prairie dogs that are not in adjacent coteries was included within Outbreak.

An additional scenario was modeled to include transmission from a secondary reservoir such as grasshopper mice. The addition of grasshopper mice increased transmission between adjacent coteries and across longer distances between non-adjacent coteries but did not affect the within-group transmission rate.

Disease Parameters

Pre-susceptible

Q1 – Proportion that never become susceptible = 0

There is no evidence of life-long resistance to *Y. pestis* infection. However, evidence for reduced virulence over generational time scales is accumulating (Rocke et al. 2012), and such resistance will be included in future implementations of this model.

Q2 – Earliest age of susceptibility (days) = 1

Q3 – Latest age of susceptibility (days) = 2

There is no evidence of maternal immunity to *Y. pestis* in prairie dogs. Therefore, young are susceptible to infection immediately after birth and may become infected within the first couple days.

Transmission to Susceptible animals

Plague is spread between prairie dogs via fleas. When a diseased prairie dog dies, it is likely that its fleas would leave the carcass and seek other hosts nearby. Reported flea abundance differs pre- versus during/post-plague epizootic and has a wide range of reported values between studies. Environmental

variables and climate (precipitation) drives flea populations, which in turn drives plague epizootics (Pauli 2006).

No plague: 39% pdogs harbor fleas with mean of 1.3 fleas/pdog (+/- 0.18)

Plague epizootic: 71% pdogs harbor fleas with 3.9 fleas/pdog (Tripp 2009)

No plague: 80% of pdogs infested with O. hirsuta; mean of 8.4-9.5 fleas/pdog

Plague epizootic: mean of 11.1 fleas/pdog

Fleas carrying plague can also be spread through the prairie dog population by the movement of diseased hosts (before they die- this is minimal), cannibalism/ contact with dead prairie dogs, infested fleas within burrows, or via the movement of other hosts, such as other rodents (grasshopper mice).

Overall prevalence of *Y. pestis* positive fleas found in prairie dog populations with plague activity is 12%. Prairie dogs infected with plague infect up to 93% of their fleas with *Y. pestis* (Engelthaler 2000), primarily during the terminal stages of the disease. Fleas collected from active prairie dogs captured in the colonies did not have *Y. pestis* positive fleas. Of fleas collected within burrows, 7% were infected with *Y. pestis*.

During plague epizootics 81% of grasshopper mice are infested with prairie dog fleas with a mean of 3.8 fleas/mouse. Mice within colonies with no plague activity have 1.6 fleas/mouse (Stapp, 2007). Unlike pdogs, grasshopper mice do not respect coterie boundaries so between coterie transmission and hence colony wide transmission is enhanced by the abundance of grasshopper mice driving epizootics . If dependant on pdog dispersal or annexation of neighboring coteries that have died from plague, infection will travel only sequentially to adjacent coteries and will not result in an epizootic.

The infectious state of fleas varies temporally with transmission probability of 0.416 on day 1, 0.111 on day 2, and 0.043 on day 3. Therefore, the farther that fleas travel before encountering a new susceptible host, the lower their infectious rate at the time of exposure.

Infector parameters:

Note: the capabilities of Infector have now been integrated into Outbreak version 2.0 (Lacy et al. 2012; available at www.vortex10.org/Outbreak.html).

Within-coterie transmission – To set the transmission rate within a family group, it was assumed that the fleas (mean 7.5; range 3.9 – 11) on an infectious (I) prairie dog would disperse from the infected host either as it was sick or when it died (over the span of three days). This would likely occur within the burrow as *Y. pestis* is not transmitted to fleas until terminal stages of the disease. Active prairie dogs captured outside of burrows even during plague activity within the colony did not carry *Y. pestis* infected fleas (Engelthaler 2000). It was assumed that each coterie member has a 50% chance of receiving one of these infected fleas over the three days that the coterie member was infectious. Thus, the daily encounter rate was 1/6. This rate was then multiplied by the transmissibility of *Y. pestis* from infected fleas on the first day (0.416) on the assumption that transfer of fleas to a susceptible host would occur quickly within a coterie. This resulted in a daily transmission probability of 0.069333 within an infected coterie.

Between(adjacent)-coterie transmission – Two scenarios for transmission between adjacent coteries were evaluated. The first was solely dependent on prairie dog movement and annexation of a disease exterminated coterie by a neighboring coterie. It was assumed that naïve prairie dogs would enter a plague infected coterie from adjacent coteries once all prairie dogs in that infected coterie died from the disease. Given a coterie size of 15 and disease duration of two days, time to complete mortality of a coterie was estimated as 30 days following initial infection. To determine the contact probability for a neighboring prairie dog we used the encounter rate of 50% per day over three days that a prairie dog is infectious (1/6 per day) similar to the rate used in the within-coterie transmission. However, since a prairie dog would likely not enter a neighboring coterie until all members of that coterie were dead, we extended this probability over 30 days to get a daily encounter rate of 0.005556. We then multiplied this rate by the transmissibility of Y. pestis from an infected flea at two days post-infection (0.11) to get the probability of transmission between adjacent coteries by prairie dogs (0.0006111).

The second scenario included grasshopper mice as a transport host to achieve a higher rate of transmission of infectious fleas to adjacent coteries –similar to what has been demonstrated in the field

and modeled previously (Salkeld et al. 2010; Webb et al. 2006). Grasshopper mice are not constrained by coterie boundaries and have been shown to visit multiple coteries within one day. We assumed an equal probability that one grasshopper mouse within an infected coterie territory would visit one of eight neighboring coteries per night, based on the spatial arrangement of the model. Once within a coterie, we assumed the mouse would encounter one prairie dog within that coterie (1/15). Combining these probabilities (1/15 * 1/8) gives the daily probability that one prairie dog encounters a grasshopper mouse. The proportion of mice infested with prairie dog fleas in colonies with plague activity has been reported at .81 and up to 93% of these may be infected with *Y. pestis* if acquired from a prairie dog carcass. Alternatively, if the fleas are picked up by elsewhere, the overall prevalence of *Y. pestis* associated in fleas is lower at 12% (Engelthaler 2000). Transmissibility of *Y. pestis* from an infected flea is considered to be 0.416 based on the assumption that grasshopper mediated flea transport will occur rapidly (within one day). Combining these probabilities [grasshopper mouse encounter (.00833) * proportion of mice infested with fleas (.81) * proportion of fleas infected with *Y. pestis* (.93) * transmissibility of the flea (.416)] results in a 0.00261 probability of transmission between adjacent coteries due to grasshopper mice. This probability was then added to the prairie dog associated transmission rate to generate a cumulative transmission rate of 0.00321 to model plague epizootics when grasshopper mice are included as a secondary reservoir.

Outbreak parameters:

Outbreak assumes that disease transmission is equally likely among any two animals in a population with no spatial structure to the disease spread. Therefore, Outbreak was used to model the transmission from an infected prairie dog to others elsewhere in the population, via transport of an infected flea by a rodent (ie, grasshopper mouse) or other reservoir that was moving through the population. It was assumed that there was a 5% chance per day (i.e., 50 prairie dogs out of the 1000 in the prairie dog population per day) that a grasshopper mouse would encounter a prairie dog within three days of visiting a non-adjacent coterie. Upon encounter, there is a 0.81 probability that the mouse is infested with prairie dogs fleas, 12% of which may be infected with *Y. pestis*. We used the lower flea infection rate of 0.12 which reflects the overall prevalence of *Y. pestis* in fleas across a colony with plague activity (Engelthaler 2000). It was assumed that the infectiousness of the flea would have dropped to the lower 0.043 probability (3 days post-infection) by the time it found a distant host. [Note: the number of long-distance transfers of fleas seems very uncertain, but the overall disease dynamics is very insensitive to

this parameter. Even if the rate is 10x higher, it will contribute rather little to the spread of the disease. The disease is maintained almost solely by the transmission between adjacent coteries.]

To model this scenario, the following Outbreak parameters were specified:

Q1 – Encounter rate was set as a fixed number (3) per day, rather than a proportion of the population, based on the number of coteries visited by a grasshopper mouse in one night (3) assuming that the mouse would encounter one prairie dog per coterie visited. This number is frequency dependent and thus would not increase with population size. Although the average encounter rate would be less than the 1 entered into the model, the lower rate was incorporated into the probability of transmission parameter.

Q2 – Probability of transmission = 0.00020898 (with 12% of fleas infected with *Y. pestis*) This value is from overall *Y. pestis* prevalence found in fleas collected in a prairie dog colony during plague epizootics (Engelthaler, 2000), and was calculated according to the following logic:

[Daily probability that a grasshopper mouse would encounter a prairie dog within three days of visiting a non-adjacent coterie (0.05) * proportion of mice infested with fleas (0.81) * proportion of *Y. pestis* positive fleas in a prairie dog colony during plague activity (0.12) * transmissibility of *Y. pestis* from flea on the third day post-infection (0.043)]

Q3 – Probability of encounter with an outside disease source = 0.0

We did not model any infection from sources that would be unrelated to the prevalence of plague within the prairie dogs themselves. Although some transmission might come from other species, the probability of such would likely be directly related to the prevalence of plague among the prairie dogs, and such transfer between host species could be subsumed under the model described above for transmission throughout the population.

Exposed

Q1 – Minimum incubation period = 4 days

Q2- Maximum incubation period = 21 days

Infectious

Q1 – Proportion that remain infectious indefinitely = 0. Prairie dogs infected with plague generally do not survive and there is no evidence for carrier states, therefore there is no probability that an individual will remain permanently infectious.

Q2 – Minimum infectious period = 2 days

Q3- Maximum infectious period = 4 days. Following development of clinical disease, prairie dogs usually die within 2-4 days.

Q4- Probability of recovery and becoming resistant = 0

Q5- Probability of returning to susceptible = 0.05. This value is calculated as 1- 0.95(probability of death) – 0 (probability of recovery).

Q6 – Probability of mortality from the infection = 0.95

Recovered/Resistant

Although some evidence for resistance to plague has been reported in prairie dogs (Rocke et al., 2012; Pauli, 2006), we chose not to include this in our model since it is not yet well understood and is therefore difficult to parameterize. For the purposes of this model, there is no recovery and acquired immunity among infected individuals so all values in this section were set to 0.

Appendix A3: Details on the sensitivity analysis routine:

To investigate the effects of spatially-explicit plague dynamics on ferret population viability directly, we ran the ferret population model (1000 replicates each) with prey availability defined according to 500 distinct artificial prey landscapes (50 replicates each). Simulation settings were varied across the seven parameters hypothesized to most influence the dynamics of plague spread (and thereby affect ferret population viability), including four spatial characteristics related to landscape size and configuration, and three prairie dog demographic traits. Spatial variables were (1) total landscape size (square areas varying from 30 to 200 km per side), (2) number of distinct subpopulations (varying from 9 to 1681 separate colonies), (3) spatial clustering of colonies (colonies configured either in a regular grid or in 3 to 10 distinct clusters), and (4) background recurrence probability of plague (mean recurrence period varying from every 2 years to every 20 years within each landscape). Prairie dog demographic variables included in the sensitivity analysis were (1) maximum intrinsic rate of growth (varying from 1.8 to 2.8), (2) intrinsic dispersal rate (intercept term from Eq. 1, varying from 0.061 to 0.105) and (3) levelof temporal variability in growth rate. Each of the 500 scenarios was selected by randomly sampling a single value from within the low-high range for each uncertain parameter (Table 1). Duplicate scenarios were discarded and replaced to ensure that each simulation was unique. Total prairie dog abundance was evenly allocated across colonies such that landscapes with more colonies had lower per-colony abundances. Colony areas were determined by assuming a density of 50 prairie dogs per hectare (following typical estimates from high-density colonies; e.g., Severson and Plumb 1998) and colony overlap was not allowed. Clustered landscapes were created by specifying 3 to 10 starting locations and selecting neighboring colony locations according to a randomized algorithm that resulted in high-connectivity prairie dog complexes with widely varying sizes and shapes. To study the effects of spatial configuration and fragmentation *per se* (Fahrig 2003), initial abundance and carrying capacity were set at 2 million individuals (approximating the initial abundanc e of the Conata/Badlands region) for all scenarios, representing sufficient prey resources to support a robust population of over 2000 black-footed ferrets in the absence of plague (assuming a ratio of 766 prairie dogs per ferret). Given that all simulated landscapes were initialized with abundance and carrying capacity of 2 million prairie dogs, larger total metapopulation areas in our simulations corresponded to lower overall prey densities, with few to many (ranging from 9 to 1681) colonies spread evenly (grid) or unevenly (clustered) throughout the landscape.

We hypothesized that ferret extinction risk would be minimized for large, diffuse metapopulations, and that more frequent spontaneous reintroductions of plague within the prairie dog metapopulation would substantially reduce ferret population viability (Table 1). We assessed the relative importance of each variable as a predictor of black-footed ferret extinction risk using a distribution-free variant of the standard random forest algorithm (Breiman 2001) implemented using the `party` package in R (Hothorn et al. 2006; Strobl et al. 2007). Random forest is a general method for building multivariate predictive models that makes few assumptions about model structure or error distributions (Strobl et al. 2009). Relationships were visualized with conditional inference trees (Hothorn et al. 2006) and conventional bivariate scatterplots.

Because dispersal rates decline with the spatial separation of subpopulations, we may infer that mean nearest-neighbor distance (as a direct measure of connectivity) would be among the best predictors of plague spread, at least for gridded landscapes (the presence of clustered complexes makes this relationship less clear). Therefore, we also assessed the relationship between ferret extinction risk and mean nearest neighbor distance among prairie dog colonies. To test univariate associations and compare variables in terms of association with ferret population viability within the sensitivity analysis, we also fitted univariate logit-linear models of black-footed ferret extinction risk as a function of each predictor variable. Univariate statistical models were fitted to the simulation output using maximum likelihood, and models were compared using the Akaike Information Criterion (AIC; Burnham and Anderson 2002).

After observing some unexpected, emergent oscillatory dynamics in the Conata landscape and in many of the artificial prey landscapes, we also examined how the seven key parameters influenced the emergence of oscillatory dynamics and the amplitude and frequency of the oscillations. We estimated the period of the dominant oscillation using sine wave regression (global prairie dog abundance modeled as an oscillating function of time) with coefficients estimated with maximum likelihood (results nearly identical to Fast Fourier Transform). Oscillatory amplitude was computed as the mean difference in abundance between significant peaks and troughs, which in turn were identified as 1-3 year time slices bounded by significant local (5-year) linear slope terms with opposite signs. Simulation scenarios were categorized as strongly oscillatory if the sine wave regression model was selected over a standard linear regression as the best model (delta AIC > 2) for ≥ 75% of simulation replicates in a given scenario and the period of the oscillation was less than 50 years in length (Supporting Materials). To assess the

potential role of plague-driven oscillatory cycles in destabilizing ferret populations, we also examined the correspondence between ferret extinction risk (and expected minimum ferret abundance) and the occurrence of oscillations.

Table 1 (same as version in main manuscript). Hypothesized influence of prairie dog variables on black-footed ferret (BFF) population viability

Variable	**Possible values**	**Hypothesized influence on black-footed ferret (BFF) population viability**
Metapopulation size (number of distinct colonies)	9, 25, 81, 169, 441, 961, 1681	Greater number of colonies will correspond to higher BFF viability as predicted by metapopulation theory (e.g., Hanski et al. 1996)
Landscape size (km per side)	30, 40, 60, 80, 100, 200	Larger and more diffuse landscapes will correspond to higher BFF viability via lower connectivity and plague transmission rates (e.g., McCallum and Dobson 2002).
Spatial clustering of colonies	Gridded, clustered	Clustered prairie dog landscapes will enable persistence of ferrets in smaller landscapes than gridded landscapes, by reducing global connectivity (and thereby plague transmission) relative to an equivalent gridded landscape.
Mean period of spontaneous plague outbreak recurrence	2, 3, 4, 5, 10, 20	Presence of multiple plague initiation events (average of 1 colony every 2 years) will reduce BFF viability relative to single plague initiation event.
Intrinsic dispersal ability	0.061, 0.073, 0.083, 0.095, 0.105	Higher dispersal tendencies will result in more plague transmission events, and therefore will lower BFF viability.
Intrinsic (maximum) rate of growth	1.8, 2.0, 2.2, 2.4, 2.6, 2.8	Higher R_{max} will correspond to faster recovery from plague and therefore higher BFF viability.

Temporal fluctuations in vital rates	5 levels from low to high (Supporting Materials)	Higher temporal variability will not influence plague spread, but will increase risk of BFF extinction after plague episodes, when BFF (and prey) abundance is lowest.

Background rate of infection

Among the variables tested in the global sensitivity analysis was the landscape-level rate of plague recurrence (in years). However, the relevant parameter in RAMAS Metapop (Akcakaya and Root 2013) was the per-population (per-colony) rate of spontaneous reinfection (set using a .PCH file, which specifies the annual probability of catastrophe for each population; see Akcakaya 2005 for more details). We converted from the specified landscape-level background rate to the population-level background rate using the following equation,

$$br_p = 1 - (1 - br_l)^{1/ncols_l},$$

Where br_p is the population-level background rate of infection, br_l is the landscape-level background rate of infection (desired level set by the sensitivity analysis), and $ncols_l$ is the number of colonies in the landscape (also manipulated as part of the sensitivity analysis . The background rate of infection was set at 0 for the burn-in period (first 10 years) and the first 10 years of the simulation (representing the plague-free period in the Conata Basin).

Landscape configuration: clustered vs. gridded

In the spatial sensitivity analysis, the number of colonies was always set as the square of a real integer value (e.g., 9, 25, 81) such that all landscapes could be arranged as grids of prairie dog colonies with the number of colonies on each side computed as sqrt(# colonies). For prairie dog metapopulations with a grid configuration, the distance between nodes in the grid was set was computed by dividing the total extent of the landscape (km per side) by (# colonies + 1) (Fig. A3-1). Center-to-center distances between

colonies (for use in determining the spatial correlation of environmental stochasticity) were computed using the Pythagorean theorem (colony centers were set at the internal nodes of the grid), and center-to-edge distances (for use in computing dispersal rates; see Appendix A1, section on Dispersal) were computed by subtracting the colony radius from the center-to-center distance. Assuming circular colonies, colony radius was computed according to the formula,

$$\sqrt{\left\{\left[\left(\frac{n_l}{ncols_l}\right)/d\right] * 0.01\right\}/\pi},$$

where n_l is the landscape abundance (set at 2 million), $ncols_l$ is the number of colonies in the landscape, and d is the maximum number of prairie dogs per ha, set at 50 per ha (see main text), and 0.01 is a conversion factor to convert from ha to km^2.

To explore the consequences of spatial aggregation of prairie dog colonies on plague spread and black-footed ferret population viability, we implemented the following clustering algorithm:

1) Divide the landscape into a fine grid
    a. Define distances between nodes (potential colony centers) such that the distances between the edges of potential colonies (assuming circular colonies with radii determined as above) are between 0.25 km and 2 km (selected randomly; typical range of inter-colony distances observed at Conata Basin study site). If the inter-colony distance is larger than that allowed by the landscape extent (determined according to the gridded colony configuration), then select a smaller inter-node distance that fits within the allowable landscape extent.
    b. Define the number of nodes per side based on the intended landscape extent (km per side divided by inter-node distance).
2) Randomly determine the number of clusters by sampling evenly from the set {4:10} .
3) Randomly determine the number of colonies in each cluster as a single multinomial draw with size set as the total number of colonies in the landscape and the probabilities assigned evenly across the number of clusters determined in the previous step.

4) Assign grid cells (uniform probability) randomly to serve as seed sites for cluster formation such that the distance between clusters is ≥10X the distance between colonies (center-to-center) where possible (constrained by the available the available landscape extent).
5) For each cluster, assign the locations of constituent colonies as follows:
    a. Beginning with the starting point (node) determined in the previous step, search for neighboring nodes that do not already host prairie dog colonies. Claim these nodes as the locations of constituent colonies.
    b. If some colony locations remain undefined and no neighboring nodes are available, randomly select a neighboring cell to serve as the new "starting location". Keep moving to new neighboring nodes until a node is identified such that at least one neighboring sites is available (currently unoccupied by a prairie dog colony).
    c. Repeat step (a), with the starting point replaced by the new focal node selected in (b).
    d. Continue until spatial coordinates have been defined for all colonies in the cluster
6) Once Cartesian coordinates have been defined for all colonies, determine center-to-edge distances (for estimating dispersal; see main text) and center-to-center distances (for estimating correlation of environmental variation) as described for gridded landscapes.

Using the center-to-center and center-to-edge distances between all pairs of colonies (gridded and clustered landscapes), dispersal and correlation matrices were computed in R following the equations presented in Appendix A and in the main text.

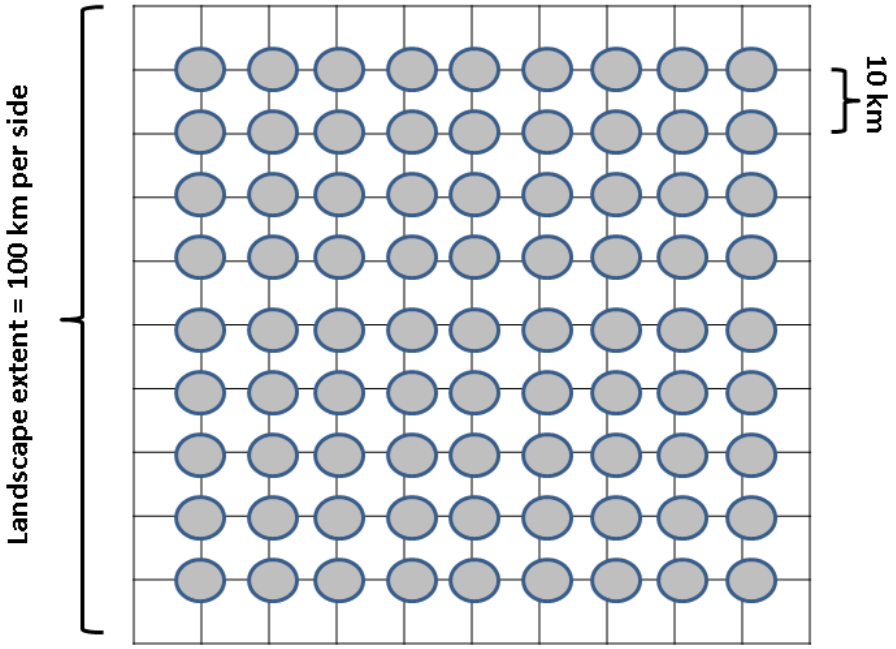

586
587

588 Figure A3-1. Illustration of the spatial arrangement of prairie dog colonies in the spatial sensitivity
589 analysis. This illustration depicts a scenario with 81 colonies and a landscape size of 100 km per side.

590

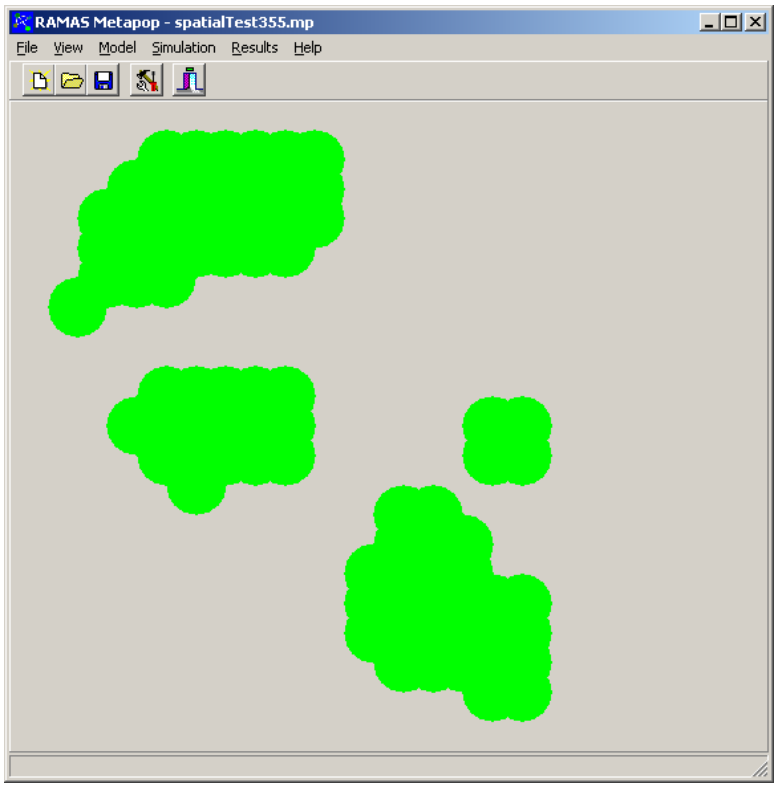
RAMAS Metapop - spatialTest355.mp
File View Model Simulation Results Help

591

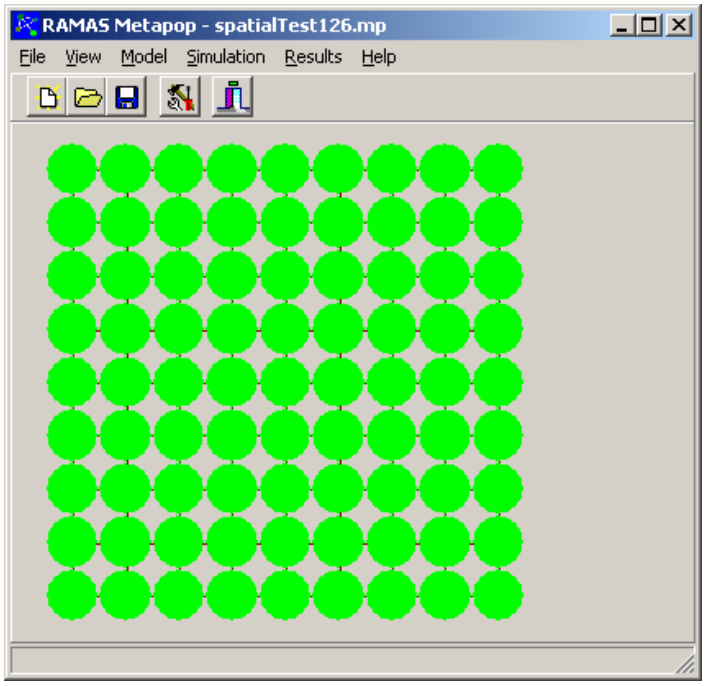
RAMAS Metapop - spatialTest126.mp
File View Model Simulation Results Help

Fig. A3-2. Example of (A) a "clustered" prairie dog landscape with 81 colonies and (B) a "gridded" prairie dog landscape with 81 colonies, visualized in RAMAS Metapop software.

Temporal environmental variability

Sensitivity of black-footed-ferret populations to variations in the temporal environmental variability of prey populations was determined in the following way:

1) For each of four distinct prairie dog transition rates (male and female survival, production rates for males and females; Table A1-1), identify five coefficients of variation (CV) ranging from low to high, with low and high levels based on Table A1-1 and central (medium) variability value identical to the mean value listed in Table A1-1.
2) For each replicate scenario in the sensitivity analysis (n = 500), randomly select a value from 1 to 5 representing low to high temporal environmental variance.
3) For each of the four transition rates identified in (1), identify the CV corresponding to the variability level selected in (2).
4) Convert to standard deviations using the mean prairie dog transition rates (Appendix A) and format as a matrix of standard deviations with the same dimensions as the transition matrix for exporting to RAMAS Metapop.

Details on analytic approach for sensitivity analysis

Sine wave regression

We used sine wave regression to diagnose the presence of an oscillatory pattern and to identify the dominant period of the oscillatory pattern in years for individual simulation trajectories. Specifically, we fit the following 6-parameter model:

$$\log(N_t) = \beta_0 + \beta_1 \cdot t + \left(\frac{a}{2}\right) \cdot \sin\left(\frac{t}{\left\{\frac{p}{2\pi}\right\}}\right) + \left(\frac{z}{2\pi}\right) + e_t,$$

where N_t represents prarie dog abundance at time t, β_0 represents an intercept term (in log abundance units), β_1 represents a linear slope term (increase or decrease in log abundance each year), a represents the oscillatory amplitude, t represents time in years, p represents oscillatory period in years, z represents an offset term in years, and e_t represents a normally distributed iid error term.

For comparison as a null, non-oscillatory baseline model (with which to test the significance of the oscillatory pattern using a likelihood ratio test or AIC model comparison), we also ran an ordinary linear regression model (three parameters):

$$\log(N_t) = \beta_0 + \beta_1 \cdot t + e_t,$$

where t, β_0, β_1, N_t, and e_t are interpreted as above.

Model fitting was performed using custom likelihood functions in R with standard numerical optimization methods (see attached R code).

Identification of peaks and troughs

Although we describe the regular increases and decreases in abundances as oscillatory, in fact the periods between peaks or troughs were somewhat irregular within simulation runs (Fig. A3-3). Therefore, the peaks and troughs identified according to sine wave regression or Fast Fourier Transform (FFT) often did not adequately predict the true locations of peaks and troughs for a given abundance trajectory (Fig. A3-3). Therefore, we developed an *ad hoc* regression-based method for identifying peaks and troughs:

1) Define moving window parameter (number of years before and after a given year of the trajectory with which to define local trends). We used a 10-year moving window in this study to characterize local trends, corresponding to 5 years before and after the focal year (candidate for designation as a "valley").
2) Define the tolerance for Type I error (α). Following standard statistical practice, we set α at 0.05.

3) Define the minimum increase or decrease in abundance (over 0.5 * moving window parameter = 5 years in this study) necessary for designation as a meaningful change. In this study, we considered an increase or decrease of 100,000 individuals or more over a 5-year period as indicative of a meaningful change (populations were initialized at 2,000,000 individuals).
4) Loop through the trajectory (*n* = 100 years). For each focal year (buffered by 0.5 X moving window parameter),
    a. Run a linear regression of log abundance over the previous 5 years (0.5 X moving window parameter). Store the p-value associated with the slope term.
    b. Run a linear regression of log abundance over the subsequent 5 years (0.5 X moving window parameter). Store the p-value associated with the slope term.
    c. Using the above linear regression models, compute the expected change in abundance over the (5-year) relevant time window before and after the focal year and the sign associated with the change (increase or decrease).
    d. If the focal year meets the following criteria, then designate the focal year as a valley:
        i. P-value for the slope term over the window prior to the focal year must be less than or equal to the specified α.
        ii. The expected abundance over the relevant window prior to the focal year must decline by an amount greater than or equal to the value specified in (3)
        iii. At least one year in the relevant window subsequent to the focal year must be associated with a significant positive slope and a meaningful increase in abundance (see above).
        iv. No other valleys identified within the moving window.

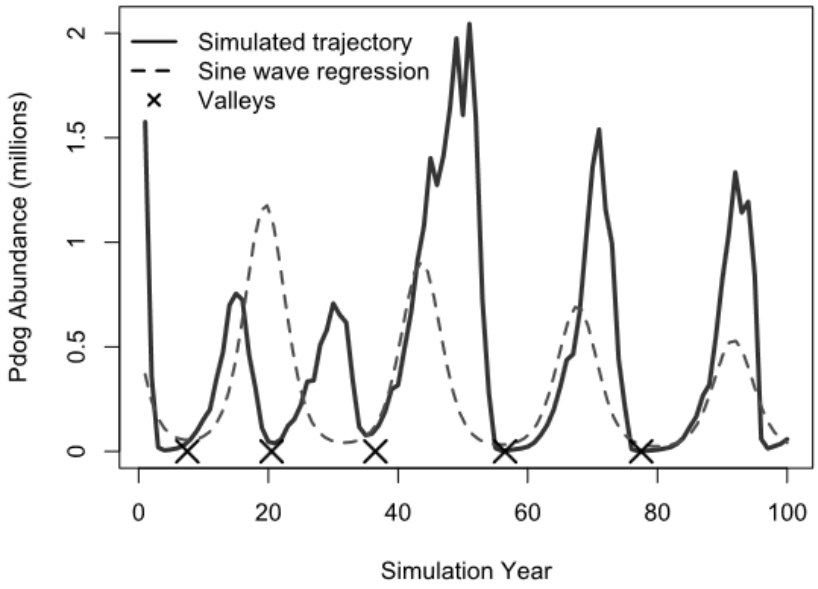
Simulated trajectory
Sine wave regression
Valleys
Pdog Abundance (millions)
0
0.5
1
1.5
2
0
20
40
60
80
100
Simulation Year

661

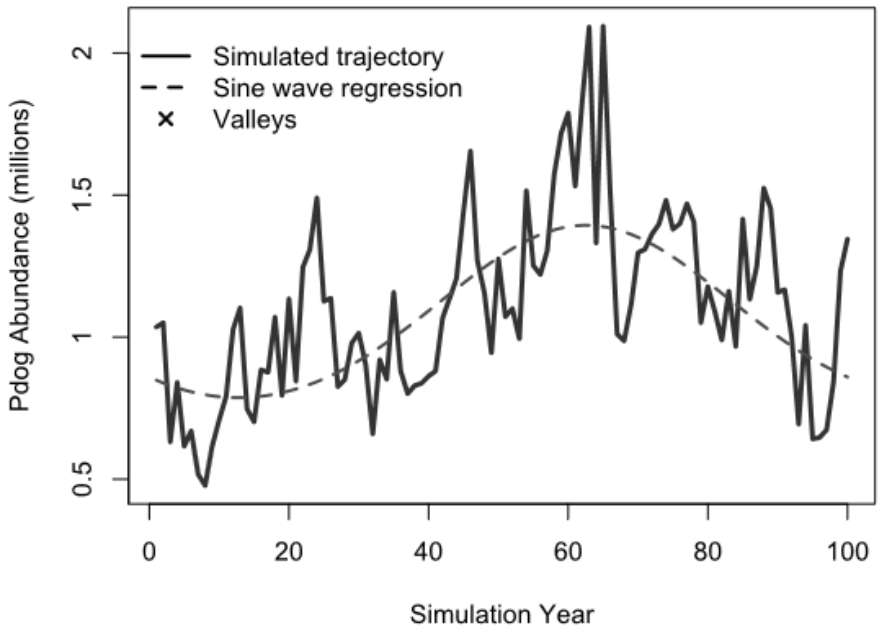
Simulated trajectory
Sine wave regression
Valleys
Pdog Abundance (millions)
0.5
1
1.5
2
0
20
40
60
80
100
Simulation Year

662

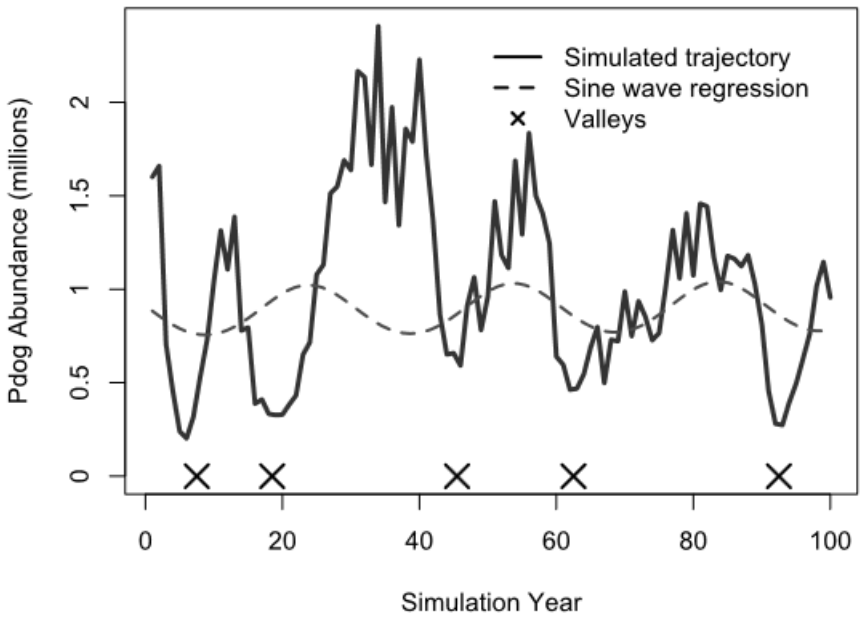

Figure A3-3. Illustration of the results of the sine wave regression and the valley identification algorithm for (A) a strongly oscillating scenario with 25 colonies with 40 X 40 km spatial extent and 5-year plague recurrence interval and (B) a non-oscillatory scenario with 169 colonies spread unevenly (clustered) in a 80 X 80 km landscape with 2-year plague recurrence interval (identified as non-oscillatory: no valleys identified and period of oscillation > 50 years) and (C) a weakly oscillatory scenario with 25 colonies distributed evenly (grid) within a 60 X 60 km landscape with a 2-year plague recurrence interval. Note that the sine wave regression did not accurately predict the locations of peaks and valleys nor did the amplitude of the sine wave regression accurately reflect the true difference in prairie dog abundance between peaks and valleys . In contrast, the regression-based algorithm was successful at identifying the true position of valleys and the true amplitude of the fluctuations.

Appendix A4: Supplementary Results and Figures

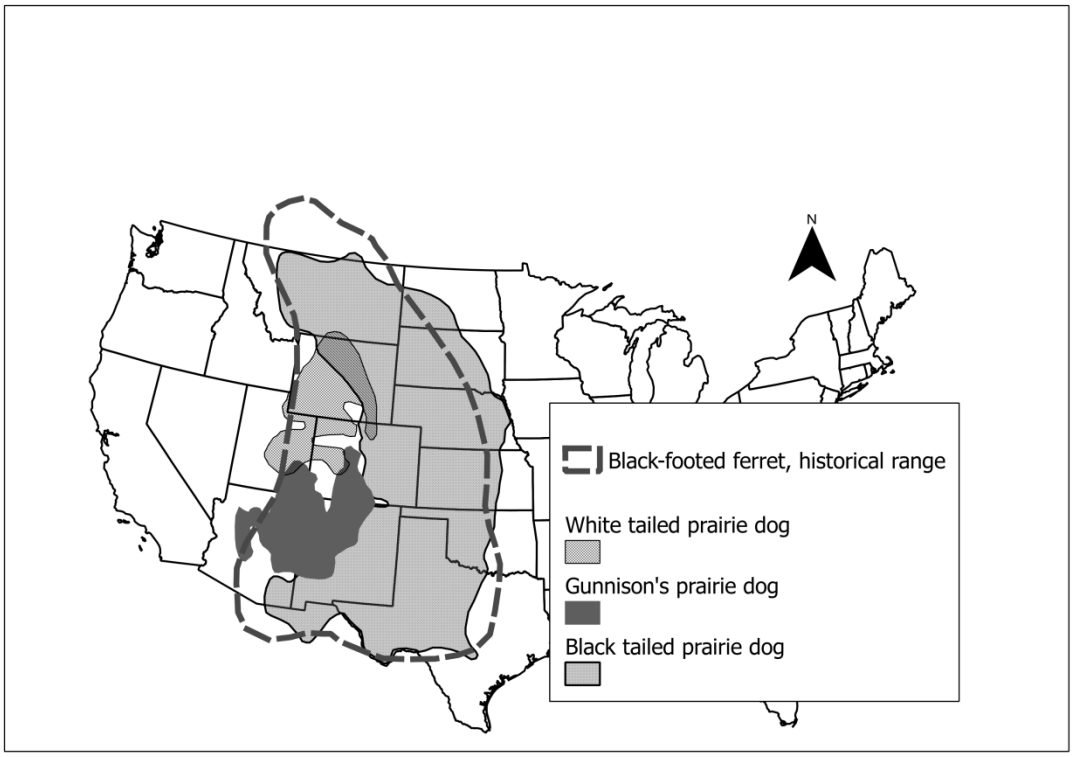

Figure A4-1. Historic range for the black-footed ferret,illustrated alongside the current ranges for the three species of prairie dogs historically consumed by black-footed ferrets (range boundaries obtained from NatureServe: http://www.natureserve.org/).

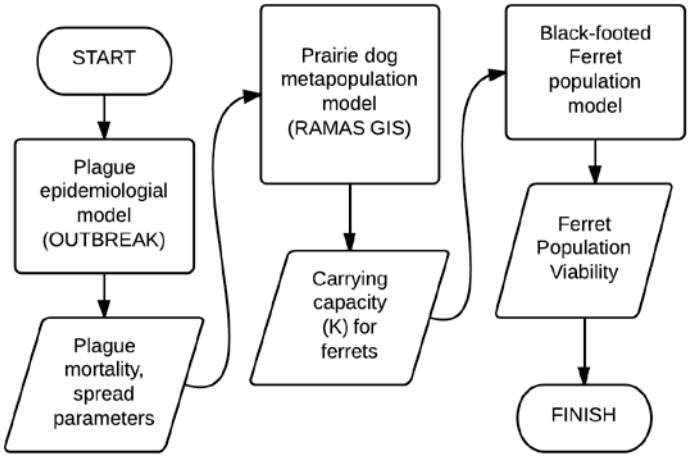

682

683 *Figure A4-2. Flow diagramof the modeling approach used in this study.*

684

Supplementary results: Conata Basin case study

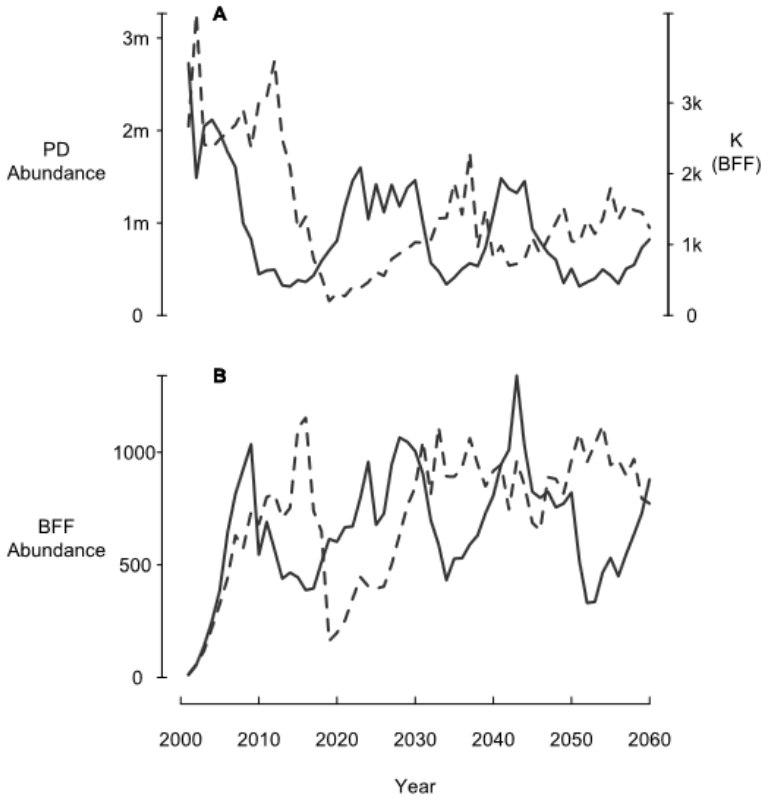

Figure A4-3. Example of oscillatory dynamics in (A) prairie dog abundance and (B) black-footed ferret abundance that emerges as a consequence of plague spread within a vast complex of 1591 prairie dog colonies in the Conata/Badlands region, South Dakota, USA. Each of the two trajectories depicted (depicted as a solid and dashed line)represent single simulation replicates drawn randomly from 1000 replicate simulations. Because oscillations among replicate simulations were not in sync, the oscillatory pattern in mean abundance across replicates appears to dampen over time.

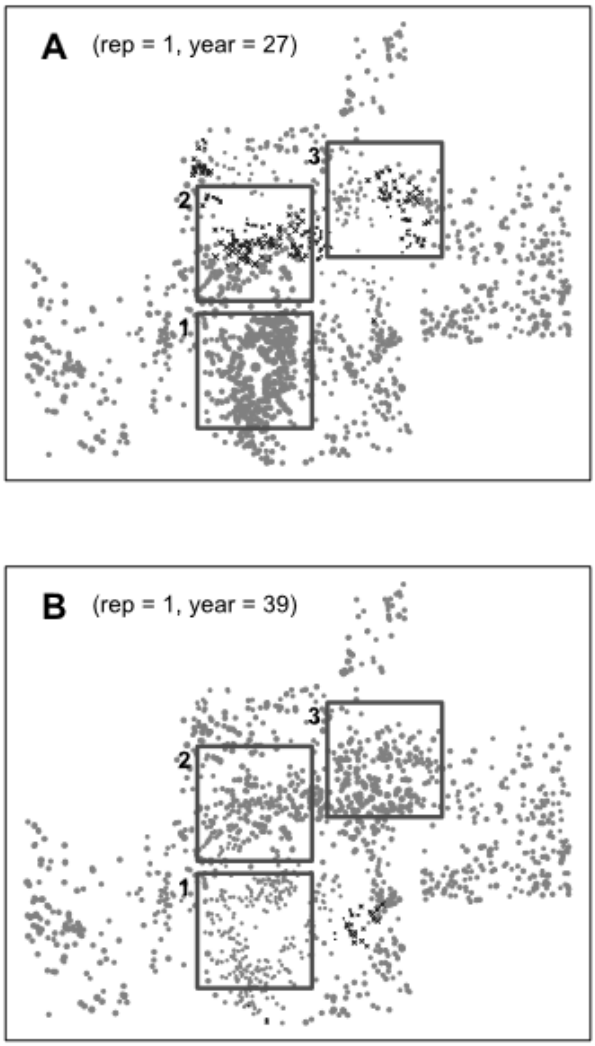

695

696 *Figure A4-4. Illustration of the spread of sylvatic plague through the prairie dog population in the*
697 *Conata/Badlands region. When plague is affecting a densely connected network of colonies within the*
698 *region, other areas are recovering and capable of supporting black footed ferrets. The key to*
699 *conservation in the face of plague may be to have enough spatial structure so that oscillatory plague*
700 *outbreak cycles are asynchronous. This figure depicts two "snapshots" from a single replicate of the*
701 *simulation model. Plague-affected colonies are illustrated with black X symbols; all other colonies are*
702 *depicted as grey dots with variable sizes corresponding to abundances.*

703

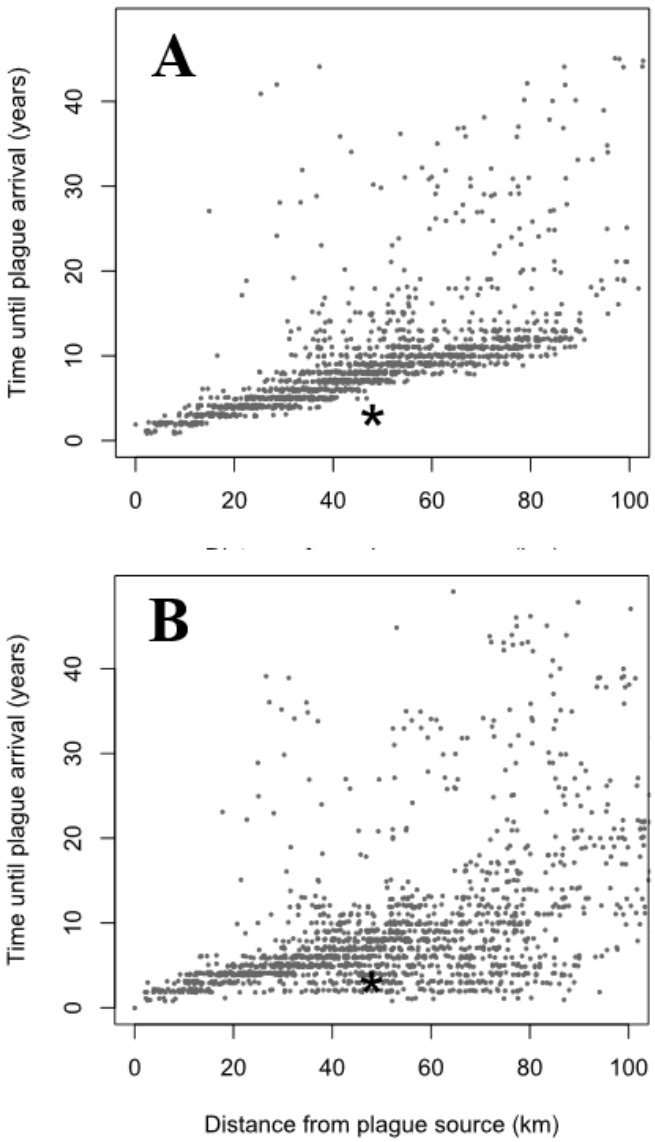

704

705 *Figure A4-5. Timing of first plague event relative to distance from the site of initial introduction (A) with*
706 *no background rate of infection (plague spread only by dispersing prairie dogs) and (B) with a 0.05% per-*
707 *population probability of "spontaneous" plague infection (plague spread by alternative long-distance*
708 *vectors such as coyotes). The asterisk in each panel represent the observed rate of spread at Conata*
709 *Basin (T.M.L., unpublished data).*

710

711 ***Animation of plague spread through the Conata-Badlands metapopulation***

712 Link to animations: (put on YouTube?? Put on Resit's website?)

713 **Supplementary results: sensitivity analysis**

714

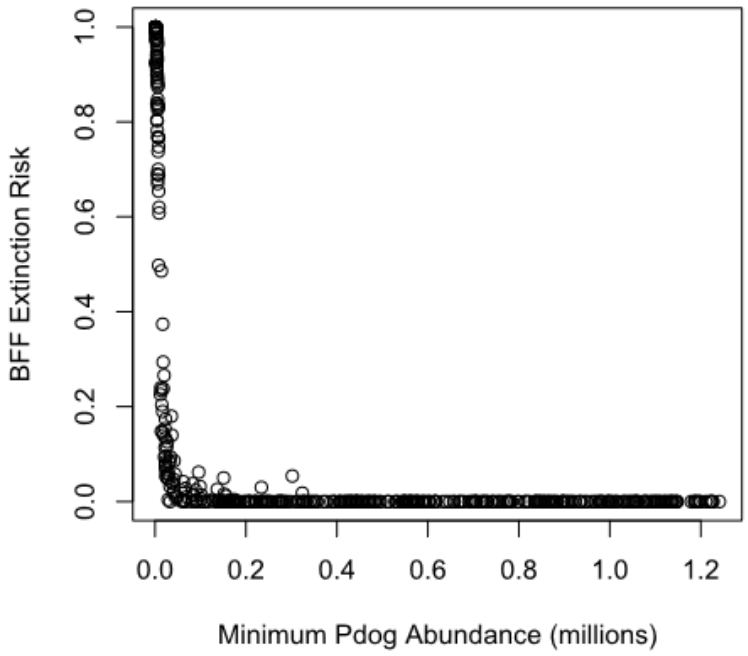

715

716 *Figure A4-6. Illustration of the very tight relationship between black-footed ferret extinction risk and the*

717 *expected minimum abundance of its obligate prey, prairie dogs*

718

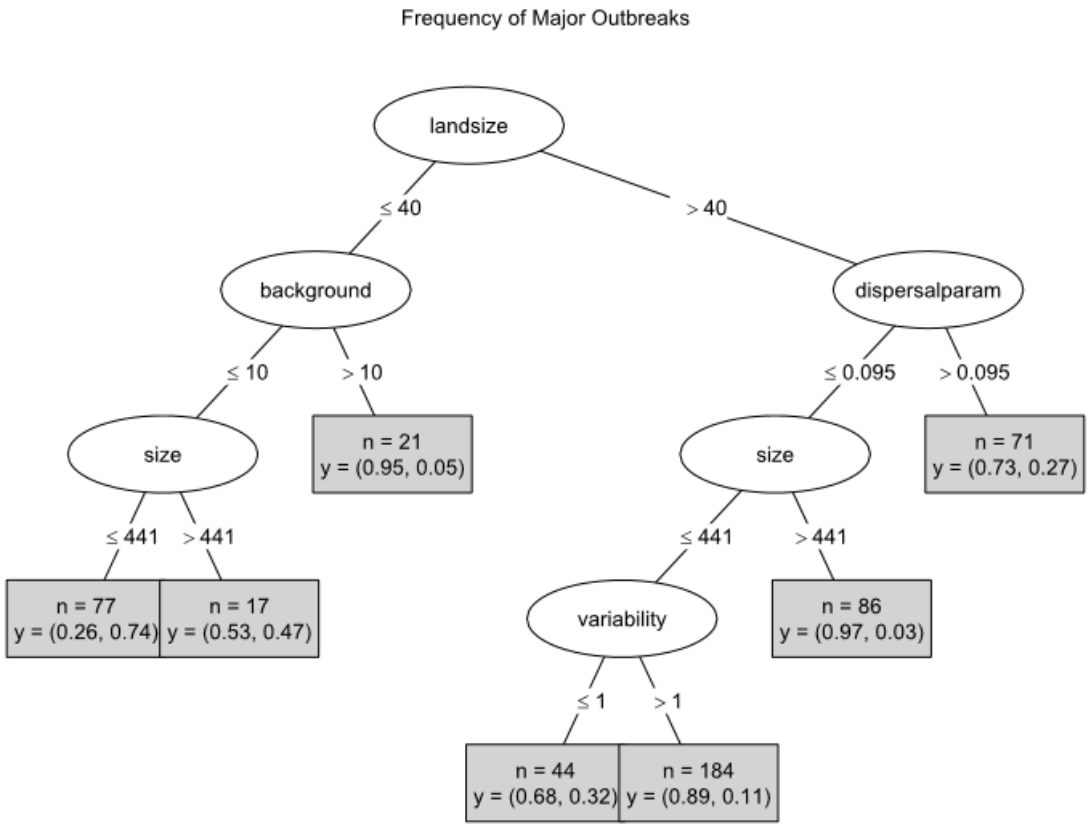
Frequency of Major Outbreaks
landsize
≤ 40
> 40
background
dispersalparam
≤ 10
> 10
≤ 0.095
> 0.095
size
n = 21
y = (0.95, 0.05)
size
n = 71
y = (0.73, 0.27)
≤ 441
> 441
≤ 441
> 441
n = 77
y = (0.26, 0.74)
n = 17
y = (0.53, 0.47)
variability
n = 86
y = (0.97, 0.03)
≤ 1
> 1
n = 44
y = (0.68, 0.32)
n = 184
y = (0.89, 0.11)

719

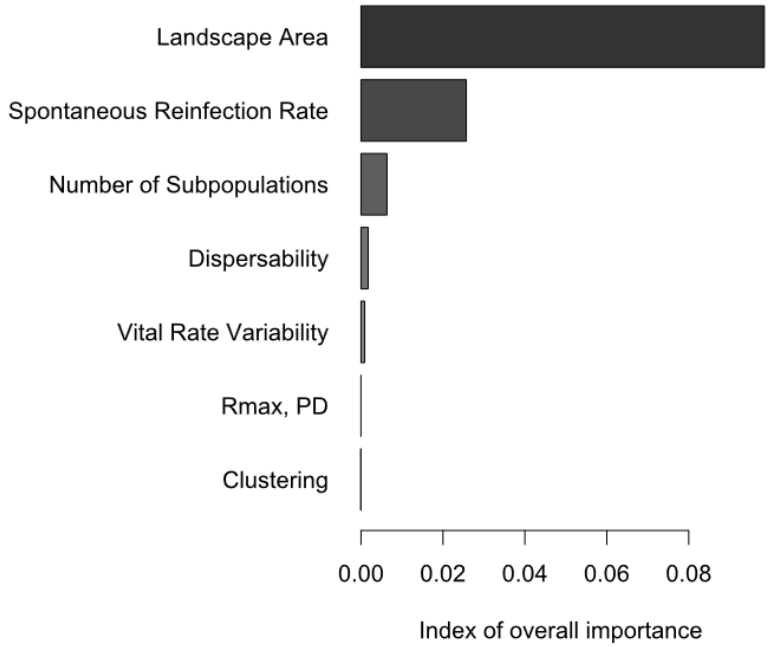
Landscape Area
Spontaneous Reinfection Rate
Number of Subpopulations
Dispersability
Vital Rate Variability
Rmax, PD
Clustering
0.00
0.02
0.04
0.06
0.08
Index of overall importance

720

Figure A4-7. (A) Binary classifaction tree (conditional inference tree: party package in R) depicting the presence of a strong oscillatory pattern as a function of the sensitivity analysis variables. "landsize" is the landscape extent (km per side), "background" is the landscape-level period of plague recurrence (years), "dispersalparam" is the mean dispersal rate between adjacent prairie dog colonies, "size" is the number of colonies in the metapopulation, and "variability" is the magnitude of temporal process variance (low to high: 1 to 5). The shaded rectangles indicate the number of simulations represented by each leaf of the classification tree, along with the mean classification: the second value listed for "y" represents the frequency of strong oscillation. Therefore, strong oscillations were observed most often for landscapes with small spatial extent (≤40 km per side; corresponding to higher densities), frequent plague recurrence, and fewer than 450 colonies. (B) Indices of variable importance from a Random Forest model (conditional inference forest: party package in R) depicting the relative importance of each sensitivity analysis variable in predicting the presence of strong oscillations.

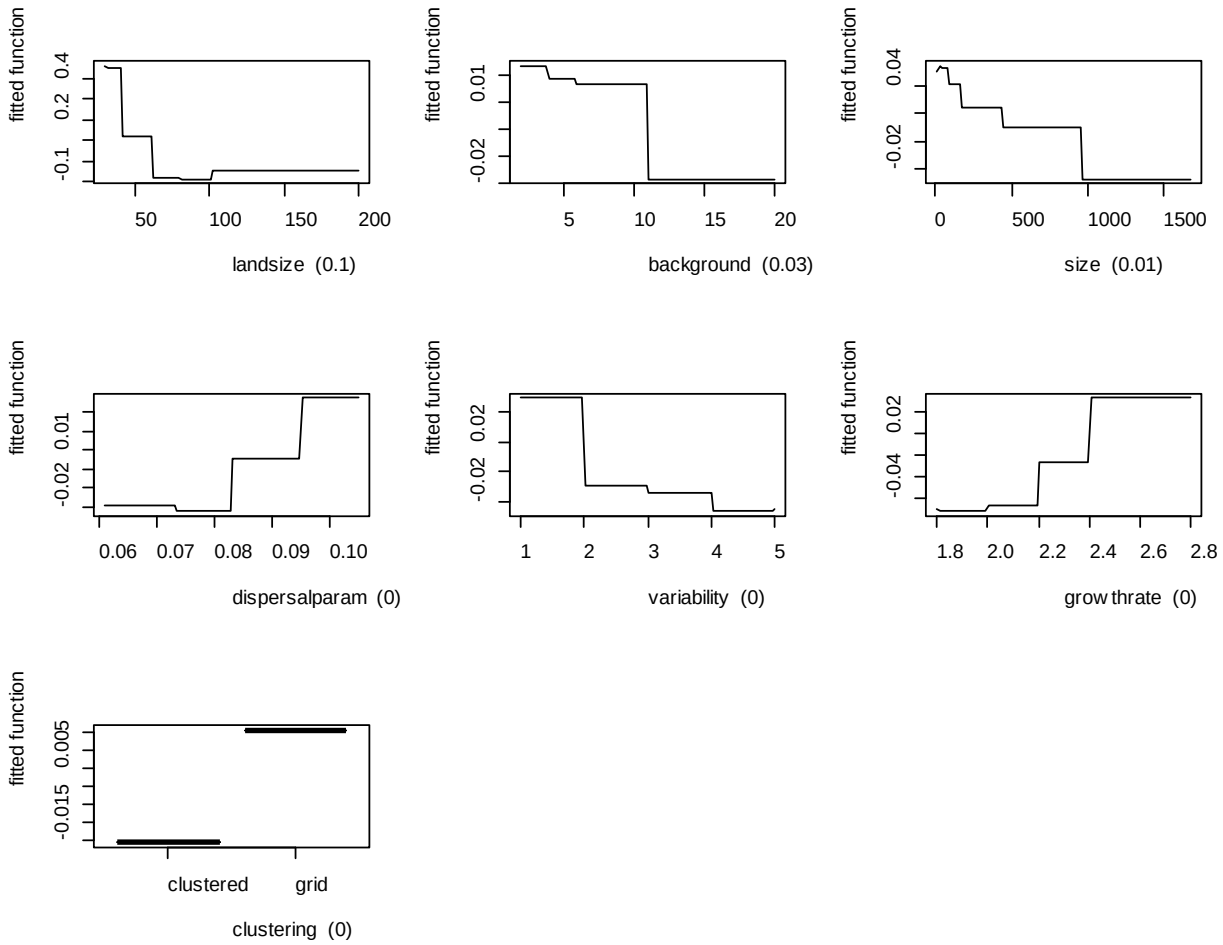

735

736 *Figure A4-8. Univariate plots illustrating the overall effect of each of the seven sensitivity analysis*
737 *variables on the frequency of a strong oscillatory pattern. Each plot is generated by using the Random*
738 *Forest model to predict the probability of oscillation across the range of each sensitivity analysis variable,*
739 *holding all other variables constant at their mean values.*

740

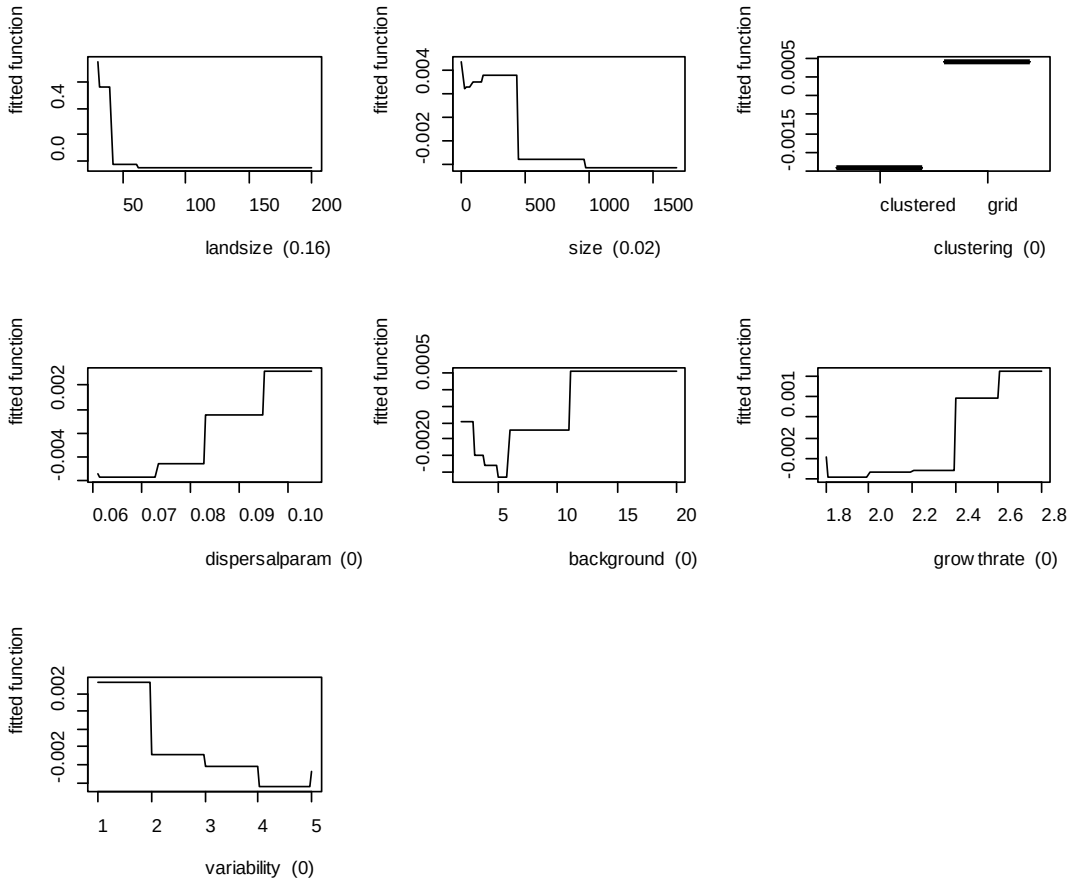

741

742 *Figure A4-9. Univariate plots illustrating the overall effect of each of the seven sensitivity analysis*
743 *variables on black-footed ferret extinction risk. Each plot is generated by using the Random Forest model*
744 *to predict the probability of oscillation across the range of each sensitivity analysis variable, holding all*
745 *other variables constant at their mean values. Note the strong similarity in the univariate responses of*
746 *ferret extinction risk and the presence of a strong oscillatory pattern (compare with Fig. A4-8).*

747

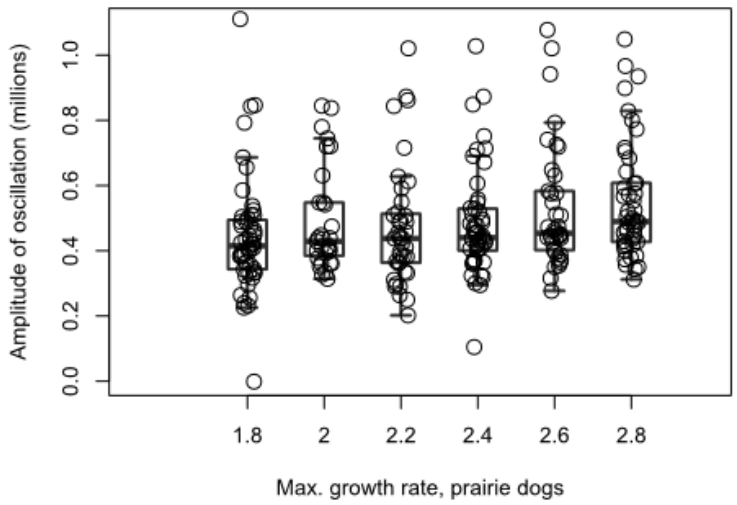

748

749 *Figure A4-10. Illustration of a weakly positive relationship between maximum intrinsic rate of growth*
750 *(R_{max}) for prairie dogs and the mean amplitude of abundance oscillations.*

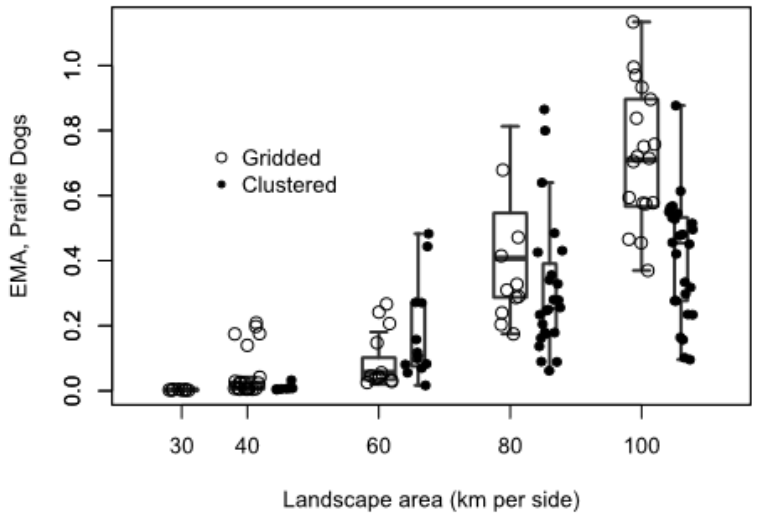

751

752 *Figure A4-11. Visualizing the effect of landscape area and colony configuration (clustered or grid) on*
753 *expected minimum abundance (EMA) for prairie dogs (in millions).*

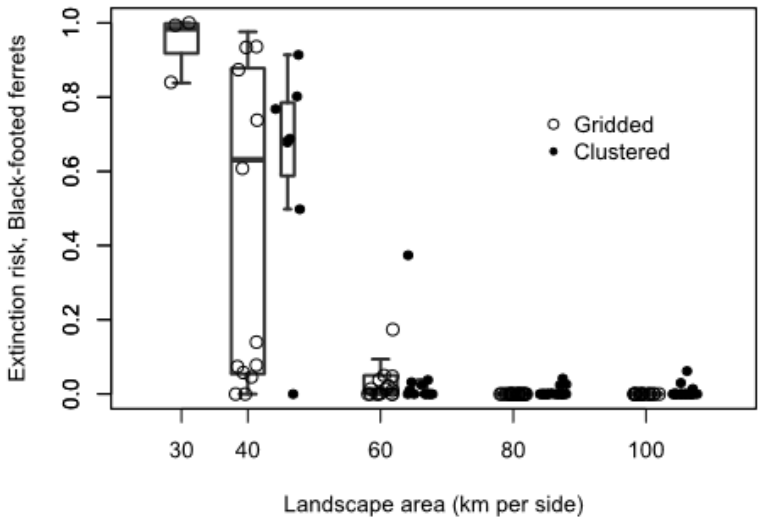

754

755 *Figure A4-13. Theoretically, clustered prairie dog landscapes could provide some benefit for black-footed*
756 *ferret conservation due to dispersal barriers. However, this effect was generally weak, and clustered*
757 *landscapes in our simulation study were generally more likely to result in lower ferret viability due to*
758 *large prairie dog complexes being devastated quickly and simultaneously.*

759

760 # REFERENCES

761 Abbott, R.C., and Rocke, T.E., 2012, Plague: U.S. Geological Survey Circular 1372, 79 p., plus appendix.
762 (Also available at http://pubs.usgs.gov/circ/1372.)

763 Akçakaya, H.R. (2002) RAMAS GIS: linking landscape data with population viability analysis . Version 4.0.
764 Applied Biomathematics, Setauket, NY.

765 Akçakaya, H.R. 2005. RAMAS GIS: Linking Spatial Data with Population Viability Analysis (version 5).
766 Applied Biomathematics, Setauket, New York.

767 Akcakaya H.R. & Root W. (2013) RAMAS METAPOP: Viability Analysis for Stage-Structured
768 Metapopulations (Version 6.0) -Applied Biomathematics. Setauket, New York.

769 Barnes, A.M. 1982. Surveillance and control of plague in the United States. P 237-270 in M.A. Edwards
770 and U. McDonnell, editors. Animal disease in relation to animal conservation. Symposia of the Zoological
771 Society of London 50. Academic Press, New York.

772 Barnes, A. M. 1993. A review of plague and its relevance to prairie dog populations and the black-footed
773 ferret. Pages 28-37 in J. L. Oldemeyer, D.E. Biggins and B. J. Miller, eds, Proceedings of the symposium
774 on the management of prairie dog complexes for the reintroduction of the black-footed ferret. US Dept.
775 Interior Biological Report 13. 96 pp.

776 Biggins, D. E, J.G. Sidle, D.B. Seery and A.E. Ernst. 2006a. Estimating the abundance of prairie dogs. Pages
777 94-107 in *Conservation of the black-tailed prairie dog: saving North America's western grasslands.* Edited
778 by John L. Hoogland. Island Press, Washington, DC.

779 Biggins, D. E., J. L. Godbey, M. R. Matchett and T. M. Livieri. 2006b. Habitat preferences and intraspecific
780 competition in black-footed ferrets. Pages 129-140 in: J. E. Roelle, B. J. Miller, J. L. Godbey, and D. E.
781 Biggins, eds. Recovery of the black-footed ferret – progress and continuing challenges. U.S. Geological
782 Survey Scientific Investigations Report 2005-5293.

783 BIGGINS, D. E., J. L. GODBEY, B. M. HORTON, AND T. M. LIVIERI. 2011. Movements and survival of black-
784 footed ferrets associated with an experimental translocation in South Dakota. Journal of Mammalogy
785 92:742–750.

786 Brannstrom, A., and D. J. T. Sumpter. 2005. The role of competition and clustering in population
787 dynamics. Proceedings of the Royal Society B 272:2065–2072.

788 Breiman, L. 2001. Random forest. Machine Learning 45:5–32.

789 Burnham, K.P. & Anderson, D.R. (2002). Model Selection and Multimodel Inference: A Practical
790 Information-Theoretic Approach, 2nd edn.. Springer Science + Business Media, LLC., Fort Collins, CO.

791 Cooper, J. and L. Gabriel. 2005. South Dakota black-tailed prairie dog conservation and management
792 plan. South Dakota Department of Game, Fish and Parks and South Dakota Department of Agriculture,
793 Pierre, South Dakota. 68p.

794 Cully J.F., et al. 2010. Disease limits populations: plague and black-tailed Pdogs. Vector Borne Zoonotic
795 Dis 10(1): 7-15

796 Cully, J. F. and E. S. Williams. 2001. Interspecific comparisons of sylvatic plague in prairie dogs. Jour.
797 Mammalogy. 82:894-905.

798 Ecke, D. H. and C. W. Johnson. 1952. Plague in Colorado and Texas. Part I. Plague in Colorado. Public
799 Health Monograph No.6. US Government Printing Office, Washington, DC. 37 pp.

800 Engelthaler DM, Gage KL (2000) Quantities of Yersinia pestis in fleas (Siphonaptera: Pulicidae,
801 Ceratophyllidae, and Hystrichopsyllidae) collected from areas of known or suspected plague activity. J
802 Med Entomol 37:422–426

803 Eskey, C.S. and V.H. Haas. 1940. Plague in the western part of the United States. U.S. Public Health
804 Service, Public Health Bulletin 254: 1-83

805 Fahrig L (2003) Effects of habitat fragmentation on biodiversity. Annu Rev Ecol Syst 34:487–515

806 Gage KL, and Kosoy MY (2005) Natural history of plague: Perspectives from more than a century of
807 research. Annu Rev Entomol 50:505–528.

808 Garrett MG, Franklin WL (1988) Behavioral ecology of dispersal in the black-tailed prairie dog. J Mamm
809 69:236–250

810 Grenier, M. B. (2008). Population biology of the black-footed ferret reintroduced into Shirley Basin,
811 Wyoming. Thesis, University ofWyoming, Laramie, USA.

812 Grenier, M.B., McDonald, D.B. & Buskirk, S.W. (2007). Rapid population growth of a critically
813 endangered carnivore. Science, 317, 779.

814 Hanski I, Moilanen A, Gyllenberg M (1996) Minimum viable metapopulation size. American Naturalist
815 147: 527–541

816 Hoogland, J. L. 1995. *The black-tailed prairie dog: social life of a burrowing mammal*. The University of
817 Chicago Press, Chicago, Illinois.

818 Hoogland, J. L. 2001. Black-tailed, Gunnison's, and Utah prairie dogs reproduce slowly. Journal of
819 Mammalogy 82:917–927.

820 Hothorn, T., K. Hornik and A. Zeileis (2006). Unbiased Recursive Partitioning: A Conditional Inference
821 Framework. Journal of Computational and Graphical Statistics, 15(3), 651--674.

822 Knowles, C., J. Proctor, and S. Forest. 2002. Black-Tailed Prairie Dog Abundance and Distribution in the
823 Great Plains Based on Historic and Contemporary Information. *Great Plains Research: A Journal of*
824 *Natural and Social Sciences*. Paper 608.http://digitalcommons.unl.edu/greatplainsresearch/608
825 (accessed 23 May 2012)

826 Lacy, R.C., Pollak, J.P., Miller, P.S., Hungerford, L. & Bright, P. (2012). Outbreak version 2.0. IUCN SSC
827 Conservation Breeding Specialist Group. Apple Valley, MN.

828 Lechleitner, R. R., L. Kartman, M. I. Goldenberg, and B. W. Hudson. 1968. An epizootic of plague in
829 Gunnison's prairie dogs (Cynomys gunnisoni) in southcentral Colorado. Ecology 49:734-743.

830 Link, V. 1955. A history of plague in the United States. Public Health Monographs 70: 1-120.

831 Livieri, T. M. 2006. Ten-year history of the Conata Basin black-footed ferret population: 1996-2005.
832 Prairie Wildlife Research, Wall, South Dakota. 49 pages.

833 Livieri, T. M. 2011. Black-footed ferret recovery in North America. Pages 157-164 in: P. Soorae, ed.
834 Global Re-introduction Perspectives: 2011. More case studies from around the globe. IUCN/SSC Re-
835 introduction Specialist Group and Abu Dhabi, UAE: Environment. 250p.

836 Livieri, T. M., D. E. Biggins, R. L. Griebel, T. Rocke and B. Powell. *In prep*. Assessing the risk of plague to
837 black-footed ferrets in Conata Basin, South Dakota.

838 Lomolino, M.V., and G.A. Smith. (2001) Dynamic biogeography of prairie dog (*Cynomys ludovicianus*)
839 towns near the edge of their range Journal of Mammalogy, 82: pp. 937–945

840 McCallum, H., Dobson, A., 2002. Disease, habitat fragmentation and conservation. Proceedings of the
841 Royal Society of London Series B-Biological Sciences 269, 2041–2049.

842 McCarthy, M. A., and C. Thompson. 2001. Expected minimum population size as a measure of threat.
843 Animal Conservation 4:351–355.

844 Pauli JN, Buskirk SW, Williams ES, Edwards WHA (2006) A plague epizootic in the black-tailed prairie dog
845 (*Cynomys ludovicianus*) J Wildl Dis 42:74–80.

846 Poland, JD and AM Barnes. 1979. Plague, pp 515-597. In JH Steele editor, CRC handbook series in
847 zoonoses. CRC, Boca Raton, FL.

848 Pollak, J.P., P.S. Miller, R.C. Lacy, L. Hungerford, P. Bright. 2008. Outbreak version 0.99. IUCN SSC
849 Conservation Breeding Specialist Group, Apple Valley, MN.

Reeve, A.F. and T.C. Vosburgh. 2006. Recreational shooting of prairie dogs. Pages 139-156 in *Conservation of the black-tailed prairie dog: saving North America's western grasslands.* Edited by John L. Hoogland. Island Press, Washington, DC.

Rocke TE, Williamson J, Cobble KR, et al. 2012. Resistance to plague among black-tailed prairie dog populations. VectorBorne Zoonot 12: 111–16.

Salkeld DJ, Salathé M, Stapp P, Jones JH (2010) Plague outbreaks in prairie dog populations explained by percolation thresholds of alternate host abundance. Proc Natl Acad Sci USA 107: 14247–14250

Sidle, J. G., D. H. Johnson and B. R. Euliss. 2001. Estimated areal extent of colonies of black-tailed prairie dogs in the northern great plains. Journal of Mammalogy 82:928-936.

Stapp P (2007) Rodent communities in active and inactive colonies of black-tailed prairie dogs in shortgrass steppe. J Mammal 88:241–249.

Strobl, C., A.-L. Boulesteix, T. Kneib, T. Augustin and A. Zeileis (2008). Conditional Variable Importance for Random Forests. BMC Bioinformatics, 9(307).

Strobl, Carolin; James Malley; and Gerhard Tutz. 2009. An Introduction to Recursive Partitioning: Rational, Application, and Characteristics of Classification and Regression Trees, Bagging, and Random Forests. Psychological Methods. 14(4): 323-348.

Stromberg, M.R., Rayburn, R.L., and Clark, T.W., 1983, Black-footed ferret prey requirements—an energy balance estimate: Journal of Wildlife Management, v. 47, p. 67–73.

Tripp DW, Gage KL, Montenieri JA, Antolin MF (2009) Flea abundance on black-tailed prairie dogs (Cynomys ludovicianus) increases during plague epizootics. Vector Borne Zoonotic Dis 9:313–321

Webb, C.T., Brooks, C.P., Gage, K.L. & Antolin, M.F. (2006).Classic flea-borne transmission does not drive plague epizootics in prairie dogs. Proc. Natl Acad. Sci. USA, 103, 6236–6241.